(50 nmol/L) was transfected into ovarian cancer cells using LipofectAMINE 2000 (Invitrogen) according to the manufacturer's instructions. The numbers of viable cells 24 to 96 h after transfection were assessed by WST assay.

Statistical analysis. Differences between subgroups were tested by the Mann-Whitney *U* test. Correlations between *CTGF* methylation or expression in primary ovarian cancers and the clinicopathologic variables pertaining to the corresponding patients were analyzed for statistical significance by χ^2 or Fisher's exact test. For the analysis of survival, Kaplan-Meier survival curves were constructed for groups based on univariate predictors, and differences between the groups were tested with the log-rank test. Differences were assessed with a two-sided test and considered significant at the $P < 0.05$ level.

Results

Array-CGH analysis of ovarian cancer cell lines. We assessed copy number alterations among the 24 ovarian cancer cell lines by array-CGH using the same batch of MCG Cancer Array-800 slides for all of them. Copy number gains and losses were seen to some degree in all 24 lines (data not shown). Figure 1*A* documents the frequencies of copy number gains and losses across the entire genome of each cell line. Our array-CGH analysis predicted frequent copy number gains for 3q and 20q and frequent losses for 4q, 13q, 15q, 17p, 18q, Xp, and Xq (Supplementary Table S3), which were mostly consistent with those of our earlier conventional CGH analysis of ovarian cancer cell lines (22) and were similar to published results of conventional CGH analyses of primary ovarian cancers (27–29).

Because the most common genetic aberrations had already been identified in ovarian cancer cell lines and primary tumors, we paid attention to more remarkable patterns of chromosomal abnormalities, such as high-level amplifications (log 2 ratio, >2) and homozygous deletions (log 2 ratio, <−2), which are likely to be landmarks of oncogenes and TSGs, respectively (Table 1). High-level amplifications were detected in two cell lines, and three clones (genes) were presented. Homozygous deletions were detected in three cell lines, and five clones (genes) were presented. Among those genes, *MTAP* and *CDKN2A/p16* located of 9p21.2, *TGFBR2* at 3p24.1, and *SMAD4* at 18q21.1 are known as TSGs inactivated in various human cancers. On the other hand, the homozygous loss at 6q23, the location of *CTGF* (Fig. 1*B*), observed in RMUG-S cells had not been documented in ovarian cancer before, prompting us to examine whether genes, including *CTGF*, located within this region might be involved in the pathogenesis of ovarian cancer.

Identification of target genes involved in homozygous deletion at 6q23.1. To define the extent of the homozygous deletion in RMUG-S cells and to identify other cell lines harboring cryptic homozygous loss in this region, we did genomic PCR experiments with 10 genes, *MOXD1, CTGF, ENPP1, ENPP3, CRSP3, ARG1, AKAP7, EPB41L2, KIAA1913*, and *L3MBTL3* (Fig. 2*B*), which are located around RP11-69I8 (Fig. 1*C*) according to information archived by genome databases.[9] We detected a complete loss of *CTGF, ENPP1, ENPP3, CRSP3, ARG1, AKAP7, EPB41L2*, and *KIAA1913* only in RMUG-S cells (4.2%), whereas *MOXD1* and *L3MBTL3* were retained in this cell line, indicating that the size of the homozygous deletion is ~2.2 Mb at maximum.

Loss of *CTGF* expression and its restoration after DNA demethylation in ovarian cancer cell lines. Next, we determined mRNA expression levels of *CTGF, ENPP1, ENPP3, CRSP3, AKAP7, EPB41L2*, and *KIAA1913* by in all 24 ovarian cancer cell lines, normal ovary, and the normal ovarian epithelial cell–derived immortalized cell line OSE-2a. We excluded *ARG1* from the analysis because our preliminary experiment (data not shown) and the information archived by the genome databases[10] showed almost no expression of this gene in normal ovary. Among seven genes we tested, *CRSP3, EPB41L2*, and *AKAP7* were expressed in most of the ovarian cancer cell lines and normal ovary (Fig. 1*C*), suggesting that these genes are unlikely to be targets for inactivation in ovarian cancer cells. On the other hand, *CTGF, ENPP1, ENPP3*, and *KIAA1913* were frequently silenced even in ovarian cancer cell lines without their homozygous loss, suggesting that the loss of expression of those genes might result from mechanisms other than genomic deletion. Because aberrant methylation in 5′ regulatory region harboring a larger than expected number of CpG dinucleotides (CpG island) is a key mechanism by which TSGs can be silenced (7), we searched for the CpG island around transcription start sites of those genes using the CpGPLOT program[11] and identified it only in *CTGF* but not in the other three genes, prompting us to focus on *CTGF* for further analyses. *CTGF* showed a complete loss of expression in the RMUG-S cell line and a reduced expression in another 12 lines without its homozygous loss (12 of 23, 52%; Fig. 1*C*). The other 11 ovarian cancer lines, normal ovary, and OSE-2a cells did express *CTGF* mRNA. Only one of the five lines that had shown a hemizygous loss around *CTGF* in array-CGH analysis exhibited a decline in the expression of this gene (data not shown).

To investigate whether DNA demethylation could restore the expression of *CTGF* mRNA, we treated ovarian cancer cells lacking *CTGF* expression with 5-aza-dCyd for 5 days. Induction of *CTGF* mRNA expression occurred after treatment with 5 μmol/L 5-aza-dCyd in HNOA and in RMG-II cells (Fig. 1*D*). In addition, we observed an enhancement of *CTGF* mRNA expression by 5-aza-dCyd given along with TSA in both lines, although treatment with TSA alone had no effect on the expression, suggesting that histone deacetylation does play some role in the transcriptional silencing of *CTGF* among methylated ovarian cancer cells. Restoration of *CTGF* expression by the treatment with 5-aza-dCyd was also observed in the rest of the ovarian cancer cell lines with reduced expression of this gene except RMUG-S (Supplementary Fig. S2*A*).

Methylation of the *CTGF* CpG island in ovarian cancer cell lines. To show the potential role of the methylation within CpG island in silencing of *CTGF*, we first assessed the methylation status of each CpG site around the *CTGF* CpG island (regions 1–3 in Fig. 2*A*) in ovarian cancer cell lines with or without *CTGF* expression and the OSE-2a cells, by means of bisulfite sequencing (Fig. 2*A*). Regions 2 and 3 tended to be extensively methylated in *CTGF*-nonexpressing cell lines (HTOA, HUOA, RMUG-L, RMG-I, HNOA, and KF28), whereas region 1 was hypomethylated in almost all cell lines tested. In addition, regions 2B, the 3′ part of region 2, and 3 are extensively methylated in some *CTGF*-expressing ovarian cancer lines (KK and OVISE), whereas region 2A, the 5′ part of region 2, tended to be hypermethylated in the nonexpressing

[9] http://www.ncbi.nlm.nih.gov/ and http://genome.ucsc.edu/

[10] http://www.ncbi.nlm.nih.gov/entrez/query.fcgi?db=unigene and http://www.lsbm.org/database/index.html

[11] http://www.ebi.ac.uk/emboss/cpgplot/

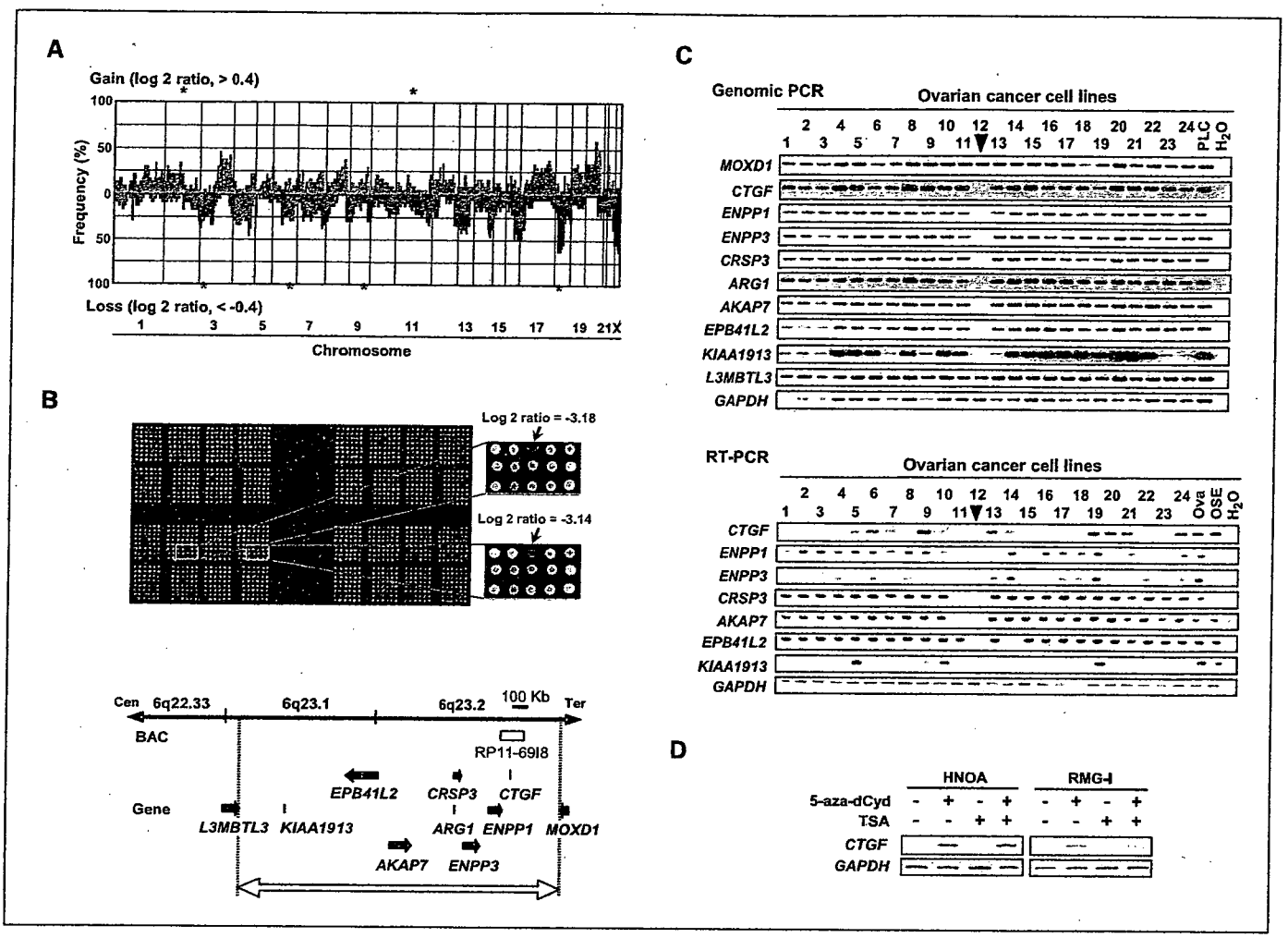

Figure 1. *A*, genome-wide frequencies of copy number gains (>0; *green*) and losses (<0; *red*) in 24 ovarian cancer cell lines. Clones are ordered as chromosomes 1 to 22 and X, and within each chromosome based on the University of California Santa Cruz (UCSC) mapping position (version May 2004). *Green asterisks*, clones with at least one high-level amplification; *red asterisks*, clones with at least one homozygous deletion (Table 1). *B*, identification of the 6q23.2 homozygous deletion in ovarian cancer cell line. *Top*, representative duplicate array-CGH image of the RMUG-S cell line. A homozygous deletion (copy number ratio as log 2 ratio) of the BAC clone at 6q23.2 was detected as a clear red signal (*red arrows*). *Bottom*, map of 6q23 covering the region homozygously deleted in the RMUG-S cell line. A BAC (RP11-69I8) was homozygously deleted in the array-CGH analysis (*vertical white bar*). Homozygously deleted region in RMUG-S cells, as determined by genomic PCR analysis (*vertical white closed arrow*). Ten genes located within this region (*red or black arrows*) show homozygously deleted or retained genes, respectively, and positions and directions of transcription. *C*, genomic and RT-PCR analyses of genes located around the 6q23 homozygously deleted region in ovarian cancer cell lines. *Top*, homozygous deletions of *CTGF*, *ENPP1*, *ENPP3*, *CRSP3*, *ARG1*, *AKAP7*, *EPB41L2*, and *KIAA1913*, but not *MOXD1* and *L3MBTL3*, were detected in one ovarian cancer cell line (RMUG-S; *arrowhead*) by genomic PCR. *1*, HT; *2*, HTOA; *3*, HUOA; *4*, KF28; *5*, MH; *6*, OVKATE; *7*, OVSAHO; *8*, KFr13; *9*, HMKOA; *10*, MCAS; *11*, RMUG-L; *12*, RMUG-S; *13*, KK; *14*, OVISE; *15*, OVMANA; *16*, OVTOKO; *17*, RMG-I; *18*, RMG-II; *19*, ES-2; *20*, W3UF; *21*, HIOAnu; *22*, HMOA; *23*, HNOA; *24*, HTBOA; PLC, peripheral leukocytes. *Bottom*, mRNA expression of *CTGF*, *ENPP1*, *ENPP3*, *CRSP3*, *AKAP7*, *EPB41L2*, and *KIAA1913* in ovarian cancer cell lines and the normal ovary (*Ova*) and normal ovarian epithelial cell–derived cell line OSE-2a (*OSE*), detected by RT-PCR analysis. *Arrowhead*, the cell line with the homozygous deletion indicated in the genomic PCR analysis. Expression of *CRSP3*, *AKAP7*, and *EPB41L2* mRNAs was observed to some degree in most ovarian cancer cell lines, whereas *ENPP1*, *ENPP3*, *CTGF*, and *KIAA1913* showed frequent silencing. Notably, 12 of the 23 cell lines (50%) without a homozygous deletion of *CTGF* showed decreased expression. *D*, results of RT-PCR to reveal restored *CTGF* expression in HNOA and RMG-I cells after treatment with 5-aza-dCyd (5 μmol/L) for 5 d with or without TSA (100 ng/mL) for 12 h.

ovarian cancer lines (HTOA, HUOA, RMUG-L, RMG-I, HNOA, and KF28) but hypomethylated in the *CTGF*-expressing ovarian cancer lines (KK, OVISE, and HTBOA) and OSE-2a cells. Consequently, methylation of region 2A was likely to be inversely correlated with the expression status of *CTGF*, suggesting that region 2A may be crucial to regulate the basal transcription level of *CTGF*.

To compare the methylation and expression status of *CTGF* in a larger number of ovarian cancer lines, we did COBRA. Consistent with the results of bisulfite sequencing, no methylated allele was detected in region 1 among most of the lines tested regardless of the *CTGF* expression status (Fig. 2*B*). On the other hand, most of the ovarian cancer cells lacking *CTGF* expression, except OVMANA and OVTOKO, had a methylated allele without an unmethylated allele in region 2, whereas most of the ovarian cancer cell lines and OSE-2a cells expressing *CTGF* had an unmethylated allele with or without methylated allele. Notably, OVISE cells expressing *CTGF* were found to have only an allele methylated in region 2 by COBRA. In this cell line, bisulfite sequencing showed that region 2B containing two *Bst*UI sites was highly methylated but region 2A was hypomethylated (Fig. 2*A*), indicating that region 2A is a critical target site for epigenetic events affecting *CTGF* expression. However, mechanisms other than DNA methylation, including

histone modification, epigenetic silencing of transcription factors or upstream components of signaling pathway activating CTGF expression, and microRNAs (30), may also contribute to the direct or indirect silencing of *CTGF*. Indeed, restoration of *CTGF* expression by TSA and/or 5-aza-dCyd was also observed in OVMANA cell line only having unmethylated allele and OVTOKO cell line having unmethylated allele and partially methylated alleles (Fig. 2*B*; Supplementary Fig. S2*B*).

Promoter activity of the sequence around the *CTGF* CpG island. Because the sequence around the *CTGF* CpG island seems to be a target for methylation and closely related to gene silencing, we tested sequences around the CpG island for promoter activity, using three fragments covering this region (fragments 1–3 in Fig. 2*A*) and three types of ovarian cancer cell lines: RMUG-S with a homozygous deletion of *CTGF*, KK expressing *CTGF*, and KF28 lacking *CTGF* expression. Because region 1 is unlikely to be a critical target for methylation, we excluded it from the analysis. Fragments 1 and 3 containing region 2A showed a remarkable increase in transcriptional activity, whereas fragment 2 not containing region 2A showed very weak activity in all types of cell lines (Fig. 2*C*), suggesting that region 2A may contain critical sequence(s) for gene silencing.

Methylation of the *CTGF* promoter region in primary ovarian cancer tumors. To determine whether the aberrant methylation of *CTGF* also takes place in primary tumors, we did MSP with primer sets targeting the sequence around the most frequently methylated sites around region 2A in a panel of 66 primary ovarian cancer tumors (Fig. 2*D*). Specificity and sensitivity of MSP and the comparison of sensitivity between MSP and COBRA were shown in Supplementary Fig. S3. Consistent with the results of the bisulfite sequencing and COBRA (Fig. 2*A* and *B*), a representative cell line lacking *CTGF* expression (RMUG-L) was methylated, whereas the *CTGF*-expressing cell line (OSE-2a) was unmethylated, as expected. We detected *CTGF* hypermethylation in 39 of the 66 primary ovarian cancer tissues (59%; Fig. 2*D*; data not shown). To confirm the results of the MSP analysis quantitatively, we did bisulfite sequencing in some of representative cases. Aberrant hypermethylation was observed in ovarian cancer tissues, which showed a methylation pattern in the MSP analysis, whereas tumors with an unmethylated pattern in the MSP analysis showed hypomethylation (Fig. 2*D*). To confirm that the methylation of *CTGF* is associated with gene silencing in primary ovarian cancer, we then examined the expression status of *CTGF* mRNA using real-time RT-PCR with cDNA prepared from 43 primary ovarian cancer tumors except for mucinous type tumors, which contain a larger amount of noncancerous cell contamination compared with other types of ovarian cancer. We found that primary tumors showing methylation of the *CTGF* region 2A by MSP expressed the gene at a significantly lower level than tumor without methylation ($P = 0.041$, Mann-Whitney U test; Fig. 2*D*), suggesting that the methylation of *CTGF* promoter and the gene silencing through this mechanism were not an artifact arising during the passage of ovarian cancer cell lines *in vitro*, but rather may be a true cancer-related event during the pathogenesis of ovarian cancer. However, no clear association between the methylation status of *CTGF* region 2A and the clinicopathologic characteristics was observed (Supplementary Table S4).

Association between expression level of CTGF and clinicopathologic characteristics in primary cases. To further clarify the clinical significance of the *CTGF* gene in ovarian cancer, the expression level of CTGF protein in primary ovarian cancer tissues was evaluated by immunohistochemistry using a CTGF-specific antibody (Supplementary Fig. S1). The results of the immunohistologic staining were classified as level 0 (negative staining), level 1 (1–10% of tumor cells stained), level 2 (10–50% of tumor cells stained), and level 3 (>50% of tumor cells stained). A high level of immunoreactivity for CTGF (level 3) was detected in normal ovarian epithelium (Fig. 3*A*). The CTGF protein was predominantly found in the cytoplasm or the membrane of normal or tumor epithelial cells. Although some ovarian cancer specimens showed high levels of CTGF (Fig. 3*B*), no or very weak immunoreactivity (levels 0 and 1) for CTGF was frequently observed in other ovarian cancer specimens (Fig. 3*C*). A low (levels 0 and 1) and high expression levels (levels 2 and 3) of CTGF were found in 84 of 103 (82%) cases and 19 of 103 (18%) cases, respectively. The relationship between the expression level of CTGF protein and the clinicopathologic characteristics is summarized in Table 2. In contrast to the *CTGF* mRNA level,

Table 1. High-level amplifications (log 2 ratio, >2.0) and homozygous deletions (log 2 ratio, <−2.0) detected in 24 ovarian cancer cell lines by array-CGH analysis using MCG Cancer Array-800

Alteration	BAC	Locus*		Cell line ($N = 24$)		Known candidate target gene†
		Chromosome band	Position	*n*	Name	
High-level amplifications (log 2 ratio, >2.0)	RP11-438012	2q14.2	chr2: 120,629,082–120,846,427	1	OVISE	*GLI2*
	RP11-300I6	11q13.3	chr11: 69,162,462–69,323,966	1	ES-2	*CCND1, FGF3*
	CTD-2234J21	11q13.3	chr11: 69,307,612–69,307,884	1	ES-2	*CCND1, FGF3*
Homozygous deletions (log 2 ratio, <−2.0)	RP11-7I16	3p24.1	chr3: 30,541,893–30,705,070	1	KFr13	*TGFBR2*
	RP11-69I8	6q23	chr6: 132,249,163–132,410,700	1	RMUG-S	None
	RP11-70L8	9p21.3	chr9: 21,732,608–21,901,258	1	HTBOA	*CDKN2A, MTAP*
	RP11-145E5	9p21.3	chr9: 21,792,634–22,022,985	1	HTBOA	*CDKN2A, MTAP*
	RP11-10I6	18q21.1	chr18: 46,348,632–46,493,352	1	RMUG-S	*SMAD4*

* Based on UCSC Genome Browser, May 2004 Assembly.
† Putative oncogenes or tumor suppressor genes located around BAC.

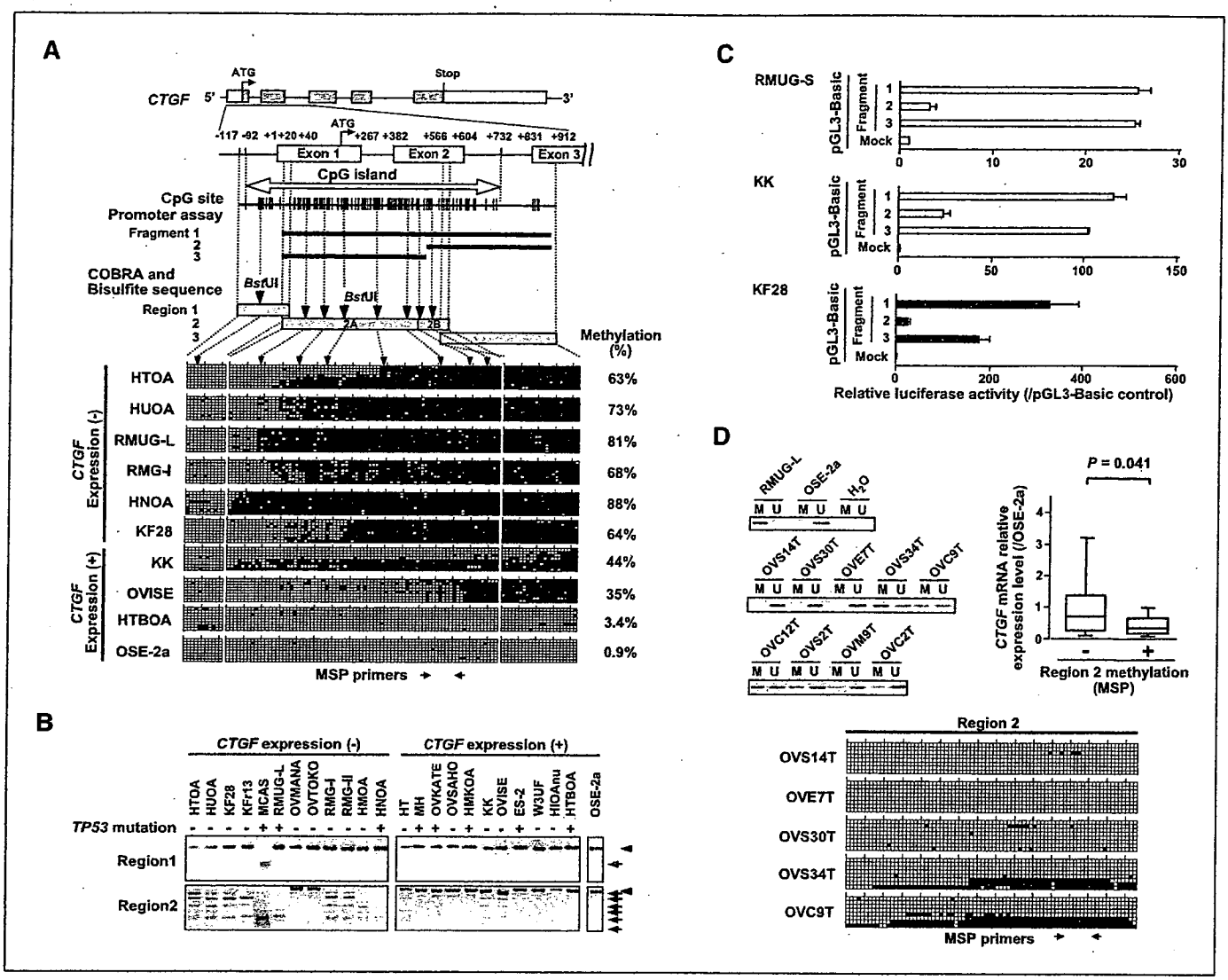

Figure 2. Methylation status of the *CTGF* CpG-rich region in ovarian cancer cell lines. *A*, schematic map of the CpG-rich region containing the CpG island (*closed white arrow*) around exon 1 of *CTGF* and representative results of bisulfite sequencing. CpG sites (*vertical ticks on the expanded axis*). Exons (*open box*). The transcription-start site is marked at +1. The fragments examined in a promoter assay (*thick black lines*). The regions examined in the COBRA and bisulfite sequencing (*horizontal gray bars*). Restriction sites for *Bst*UI (for the COBRA; *black downward arrowheads*). Representative results of bisulfite sequencing of the *CTGF* CpG-rich region examined in *CTGF*-expressing ovarian cancer cell lines (+) and *CTGF*-nonexpressing ovarian cancer cell lines (–). Each square indicates a CpG site: *open squares,* unmethylated; *solid squares,* methylated. PCR primers for MSP (*arrows*). *B,* representative results of the COBRA of the *CTGF* CpG island in ovarian cancer cell lines after restriction with *Bst*UI. *Arrows,* fragments specifically restricted at sites recognized as methylated CpGs; *arrowheads,* undigested fragments indicating unmethylated CpGs. *C,* promoter activity of the *CTGF* CpG-rich region. pGL3-Basic empty vectors (mock) and constructs containing one of three different sequences around the highly methylated region of *CTGF* (fragments 1–3 with a 157, 584, and 346 bp size, respectively, in *A*) were transfected into RMUG-S, KK, and KF28 cells. Luciferase activity was normalized versus an internal control. *Columns,* mean of three separate experiments, each done in triplicate; *bars,* SD. *D, top left,* representative results of a MSP analysis of the *CTGF* promoter region in primary ovarian cancer tissues. Parallel amplification reactions were done using primers specific for unmethylated (*U*) or methylated (*M*) DNA. *Top right,* correlation between methylation status of *CTGF* determined by MSP and mRNA expression status determined by RT-PCR in 43 primary tumors except for mucinous type tumors. Statistical analysis used the Mann-Whitney *U* test. *Horizontal bars in the boxes,* median values; *vertical bars,* range; *horizontal boundaries of the boxes,* first and third quartiles. *Bottom,* methylation status of the *CTGF* promoter region determined by bisulfite sequencing in tumor samples. *Arrows,* the positions of primers for MSP.

CTGF protein expression was not clearly associated with the methylation status of *CTGF* region 2, even in tumors other than mucinous type tumors (P = 0.215, Fisher's exact test; data not shown). CTGF protein expression was significantly associated with tumor stage: ovarian cancer tended to lack CTGF expression in the earlier stages (stages I and II) but tended to exhibit CTGF expression in the advanced stages (stages III and IV; P = 0.027, χ^2 test). CTGF protein was also differentially expressed among histologic subtypes. However, no significant relationship was found between the level of CTGF expression and the age of patients, the result of surgery, or the result of peritoneal cytology. In overall survival, no significant difference was observed between the patients with lower levels of CTGF and those with higher levels of CTGF in all stages and in stage III and IV disease (P = 0.158 and 0.148, respectively, log-rank test; data not shown). In stage I and II disease, however, no deaths occurred in patients with higher levels of CTGF expression during the study period, whereas 17.5% (10 of 57 cases) of patients with lower levels of expression died, although a statistical analysis could not be done due to no deaths in one group (Fig. 3*D*). Those findings suggest

that the incidence of the inactivation of CTGF and its role in tumorigenesis may differ with the stage and/or histologic subtype of this disease.

Suppression of cell growth induced by CTGF in ovarian cancer cells. The frequent silencing of *CTGF* in cell lines and primary tumors of ovarian cancer suggests that CTGF is likely to be a functional tumor suppressor for this disease. To investigate whether restoration of CTGF expression would suppress growth of ovarian cancer cells in which the gene had been silenced, we did colony formation assays using an expression construct of the full-coding sequence of *CTGF* (Fig. 4*A*). Two weeks after transfection and subsequent selection of drug-resistant colonies, the numbers of larger colonies produced by *CTGF*-transfected cells decreased compared with those of cells containing empty vector, regardless of mutation status of the *TP53* gene (Fig. 2*B*).

To avoid a nonspecific toxicity by forced expression of CTGF, we assessed the effect of recombinant human CTGF on growth of the nonexpressing ovarian cancer cells (Fig. 4*B, top*). Treatment with recombinant CTGF for 72 h reduced cell viability in HNOA and HMOA cell lines compared with vehicle (PBS) alone. In FACS analysis using HMOA cell line (Fig. 4*B, bottom*), treatment with recombinant CTGF resulted in an accumulation of cells in G_0-G_1 phase and a decrease in S and G_2-M phase cells but no increase in sub-G_1 phase cells compared with vehicle alone, suggesting that CTGF may arrest ovarian cancer cells at the G_1-S checkpoint (G_0-G_1 arrest) without inducing apoptosis.

To further examine the mechanisms of CTGF-induced growth inhibition in ovarian cancer cells, we investigated the effect of CTGF on EGF-dependent phosphorylation of ERK1/2 in HMOA cell line because (*a*) the overexpression of the EGF receptor is associated with poor prognosis of ovarian cancer (31) and (*b*) the suppressive effect of CTGF overexpression on EGF-dependent phosphorylation has been reported in non–small cell lung cancer (NSCLC) cell line (16). In serum-starved HMOA cells, ERK1/2 was remarkably phosphorylated with EGF treatment and the level of phosphorylation was decreased by pretreatment with CTGF (Fig. 4*C*).

To confirm a growth-suppressive effect of CTGF, we knocked down endogenously expressed CTGF by transient transfection of *CTGF*-siRNA to KK and ES-2 cell lines retaining expression of CTGF (Fig. 4*D*). Transfection of *CTGF*-siRNA accelerated cell growth in those cell lines compared with *Luc*-siRNA–transfected counterparts. Because transfection of *CTGF*-siRNA to RMUG-S cell line lacking *CTGF* expression showed no effect on cell growth compared with *Luc*-siRNA, growth-promoting effect of *CTGF*-siRNA observed in KK and ES-2 cells may not be caused by off-target effects of siRNA used in this study.

Discussion

In this study, we identified a homozygous deletion of *CTGF* at 6q23.2 in ovarian cancer cell lines by array-CGH analysis using an in-house BAC array. Expression of *CTGF* was detected in normal ovary and a normal ovarian epithelial cell–derived cell line but frequently silenced through methylation of CpG sites around the *CTGF* CpG island exhibiting promoter activity in our panel of ovarian cancer cell lines, suggesting that *CTGF* may be one of targets for inactivation in ovarian cancer, although possible involvement of other target gene(s) for the homozygous loss at 6q23.1 remains unclear. Hypermethylation of the *CTGF* promoter region was frequently detected in primary ovarian cancers. Lower CTGF protein levels were frequently observed in primary ovarian cancers, although the clinical significance of CTGF expression might differ among disease stages and histologic subtypes. In addition, the transient transfection of *CTGF* or treatment with recombinant CTGF had an inhibitory effect on growth of *CTGF*-nonexpressing ovarian cancer cells, whereas knockdown of CTGF using siRNA accelerated growth of

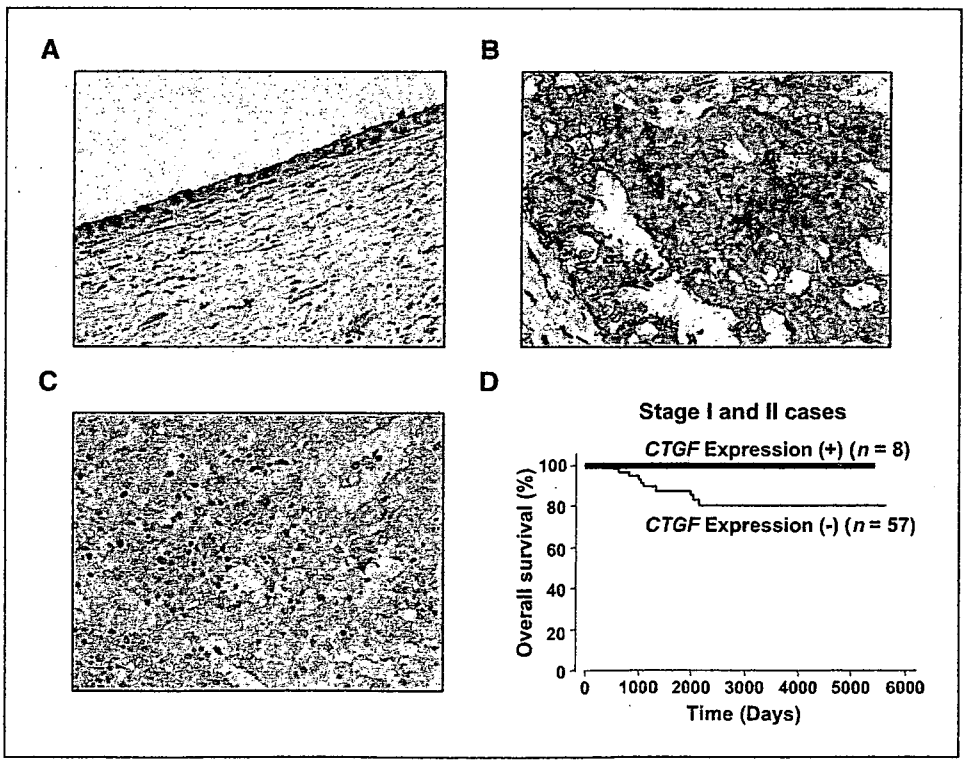

Figure 3. Immunohistochemical analysis of CTGF expression in primary ovarian cancer tumors. *A*, representative CTGF immunohistochemical staining of normal human ovarian epithelial cells. High CTGF expression is shown in normal ovarian epithelial cells. Magnification, ×200. *B* and *C*, representative CTGF immunohistochemical staining of primary ovarian cancer cells. High (*B*) or almost no (*C*) expression of CTGF was observed in primary ovarian cancer cells. In normal epithelial cells and ovarian cancer cells, CTGF is localized distinctly in the apical cytoplasm. Magnification, ×200. *D*, Kaplan-Meier curve for overall survival rates of patients with stage I and II ovarian cancer. There were no deaths in patients with stage I and II ovarian cancers showing higher CTGF levels.

Table 2. Correlation between clinical background and expression of CTGF protein

	n	Expression of CTGF*	*P*†
		n (%)	
Total	103	19 (18)	
Age (y)			
<60	71	15 (21)	0.388
≥60	32	4 (13)	
FIGO stage			
I and II	66	8 (12)	**0.027**
III and IV	37	11 (30)	
Histologic type			
Serous	42	8 (19)	**0.029**
Mucinous	15	7 (47)	
Clear cell	34	2 (6)	
Endometrioid	12	2 (17)	
Optimal surgery (cm)			
Optimal (<2)	82	16 (20)	1.000
Suboptimal (≥2)	14	2 (14)	
Unknown	7	1 (14)	
Peritoneal cytology			
Positive	48	11 (23)	0.387
Negative	50	8 (16)	
Unknown	5	0 (0)	
Methylation‡			
Positive	33	6 (18)	0.739
Negative	22	5 (23)	
Unknown	48	8 (17)	

NOTE: Statistically significant values are in boldface type.
* CTGF protein expression was evaluated by immunohistochemical analysis described in Materials and Methods.
† *P* values are from χ^2 or Fisher's exact test and were statistically significant when <0.05 (two sided).
‡ Methylation status was determined by MSP target for region 2A described in Materials and Methods.

CTGF-expressing ovarian cancer cells. These results suggest that loss of epigenetic inactivation of CTGF plays a pivotal role in the tumorigenesis of ovarian epithelial cells.

CTGF is a member of the CCN family, which comprises CTGF, cysteine-rich 61 (Cyr61/CCN1), nephroblastoma overexpressed (Nov/CCN3), Wisp-1/elm1 (CCN4), Wisp-2/rCop1 (CCN5), and Wisp-3 (CCN6). Among them, CTGF is believed to be a multifunctional signaling modulator involved in a wide variety of biological or pathologic processes, such as angiogenesis, osteogenesis, and renal and skin disorders (32–35). In carcinogenesis, CTGF was shown to be a positive regulator: the level of CTGF expression is positively correlated with bone metastasis in breast cancer (36), glioblastoma growth (37), a poor prognosis in esophageal adenocarcinomas (38), the aggressive behavior of pancreatic cancer cells (39), the invasive melanoma (40), and prognosis of chondrosarcoma (41). On the other hand, there is a body of evidence showing antigrowth (16, 42, 43) or antimetastatic (15) activity of CTGF in cancer cells and decreased CTGF expression in the aggressive or metastatic phenotype in various cancers, such as breast, colon, and NSCLCs (15, 16, 45). Given our results showing a tumor-suppressive function of CTGF, the role of CTGF in various cancers seems to vary considerably, depending on the tissues involved, although the exact mechanism has not yet been clarified. The question of how the tissue context is able to determine the action of CTGF in carcinogenesis deserves further investigation.

CTGF is located at 6q23.1, a chromosomal region that is rarely involved in copy number losses (22, 27–29). Indeed, most of the ovarian cancer cell lines used in this study showed normal DNA copy numbers around this region. Among 12 cell lines that showed reduced expression of *CTGF*, 9 lines had promoter hypermethylation, only 1 line showed both hemizygous deletion around this gene and promoter hypermethylation, whereas 2 lines showed neither, suggesting that the inactivation of CTGF might occur frequently through methylation of both alleles during the tumorigenesis of ovarian cancer. DNA methylation around the *CTGF* gene has also been reported in other cancers, such as hepatocellular carcinoma (17, 18) and colon cancer cell lines (19), suggesting that *CTGF* might be a universal target for methylation in various types of cancers. However, (*a*) some ovarian cancer cell lines showed reduced *CTGF* expression without DNA methylation and (*b*) silencing of CTGF protein expression occurs more frequently compared with DNA methylation of the *CTGF* gene in primary ovarian cancer, suggesting that mechanisms other than DNA methylation also contribute to silencing of CTGF in ovarian cancer. Recently, miR-17-92, especially miR-18, was shown to be responsible for CTGF down-regulation in Myc-transduced RAS-transformed mice colonocytes (30). Therefore, further analyses will be needed to clarify all mechanisms for silencing CTGF expression and determine the functional significance of each mechanism in primary ovarian cancer.

In our promoter assays, the *CTGF* CpG island around exons 1 and 2, especially fragment 3 from exon 1 to the middle of exon 2, whose methylation status was inversely related with expression status in ovarian cancer cells, showed clear promoter activity, whereas fragment 2 from the middle of exon 2 to exon 3, which was highly methylated in ovarian cancer cells regardless of expression status, showed weaker promoter activity. It was reported that the commonly methylated region within the *CTGF* CpG island starts from the middle of exon 1 and its methylation seems to be inversely correlated with *CTGF* expression in hepatocellular carcinoma cell lines (17, 18), and exonic methylation is observed in colon cancer cell lines with increased expression of *CTGF* caused by 5-aza-dCyd treatment (19), although methylation status of CpG sites through the entire CpG island and its correlation with gene expression was not clearly shown (17–19). Those results suggest that methylation of CpG sites within fragment 3/region 2A might be responsible for the silencing of *CTGF*, although few studies have shown that promoter activity can occur in fragments, especially CpG islands, not containing a 5′ sequence around transcription start sites (9, 46–48).

In the present study, little or no immunoreactivity for CTGF protein was observed in most primary ovarian cancers, especially in the earlier stages, which is contrary to the previously reported finding that low-level immunoreactivity was usually observed in advanced stage of colorectal cancers (15). In the earlier stages of ovarian cancer, moreover, patients with tumors showing lower CTGF immunoreactivity tended to have a worse survival rate than those showing higher levels of expression. Because we showed that (*a*) normal ovarian epithelia and immortalized ovarian epithelial cell–derived cell line express CTGF and (*b*) induction of *CTGF* expression or treatment of recombinant CTGF inhibited growth of *CTGF*-nonexpressing ovarian cancer cells, it is suggested that frequent silencing of *CTGF* occurred as an early event in ovarian

cancers at least partly through promoter methylation may contribute to the progression to an advanced stage. In the advanced stages, on the other hand, *CTGF* expression might be restored and contribute to more malignant phenotypes, such as invasion and metastasis, although the number of cases was too small to provide any conclusive results in the statistical analysis. In a breast cancer model (36), *CTGF* was identified as one of the genes contributing to bone metastagenicity, and its expression was transcriptionally induced by transforming growth factor β (TGFβ), which can have direct pro-oncogenic effects on tumor cells by stimulating their invasion and metastasis at least partially by inducing epithelial-to-mesenchymal transition in the later stages of carcinogenesis, when cancer cells have become insensitive to TGFβ-induced growth inhibition and apoptosis (36, 49). Therefore, it is possible that CTGF expression might be induced or restored by TGFβ to acquire an invasive/metastatic phenotype in advanced ovarian cancers without *CTGF* methylation. Because the silencing of *CTGF* occurs in a subset of ovarian cancer and may affect various biological functions in a stage-dependent and/or histologic subtype-dependent manner, evaluation of the methylation and/or expression status of *CTGF* with disease stage and/or histologic subtype might be useful for predicting the progression or

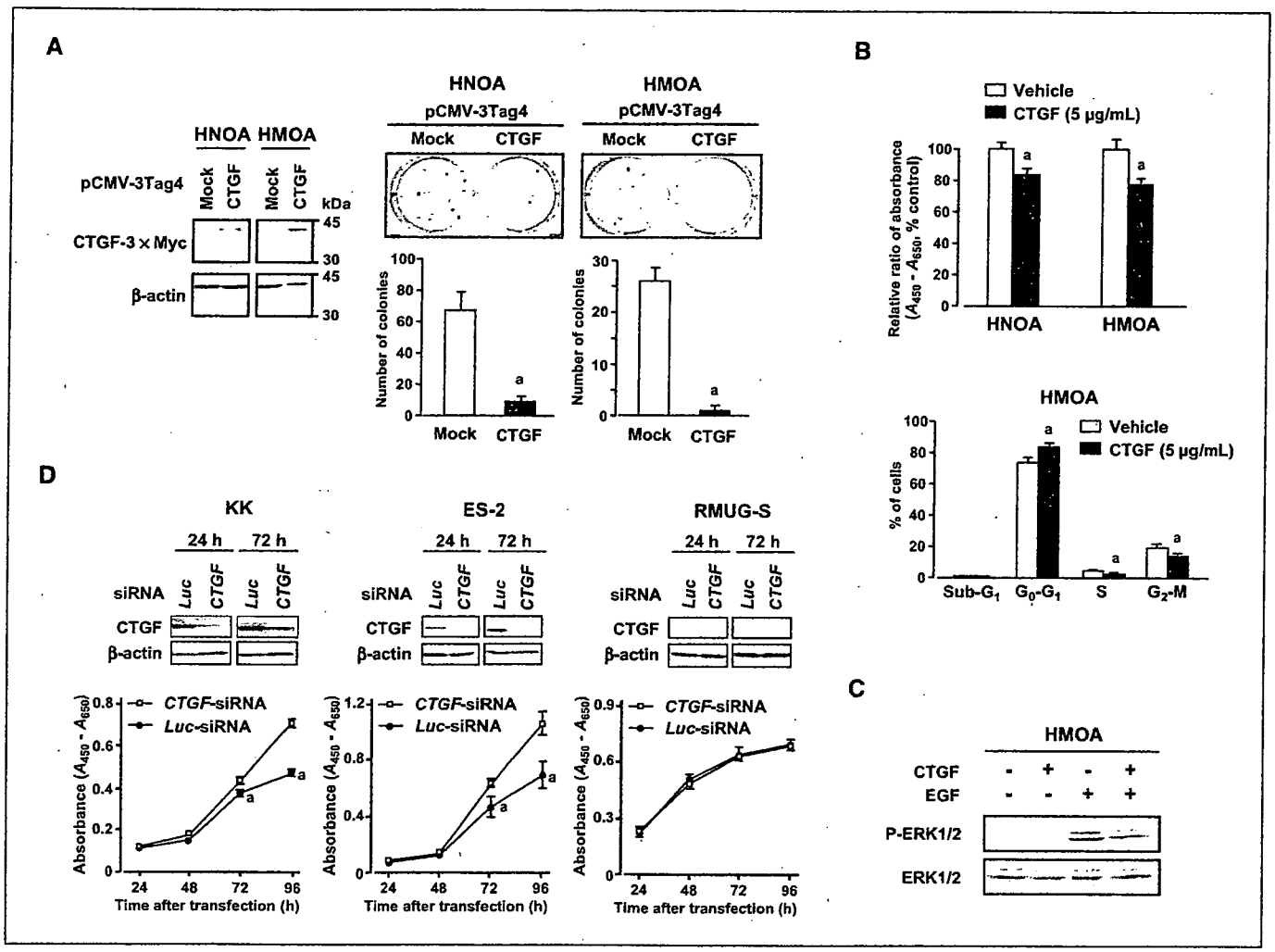

Figure 4. *A*, effects of restoration of CTGF expression on growth of ovarian cancer cells. Colony formation assays were done using ovarian cancer cell lines lacking expression of *CTGF*. Cells were transiently transfected with a Myc-tagged construct containing *CTGF* (pCMV-3Tag4-CTGF), or empty vector (mock), and selected for 2 wks with appropriate concentrations of G418. *Left*, Western blot prepared with 10 μg of protein extract and anti-Myc antibody, showing that cells transiently transfected with pCMV-3Tag4-CTGF expressed Myc-tagged CTGF. *Right, top*, 2 wks after transfection and subsequent selection of drug-resistant colonies, the colonies formed by *CTGF*-transfected cells were less numerous than those formed by mock-transfected cells. *Right, bottom*, quantitative analysis of colony formation. Colonies >2 mm were counted. *Columns*, mean of three separate experiments, each done in triplicate (histogram); *bars*, SD. *a*, $P < 0.05$, statistical analysis used the Mann-Whitney *U* test. *B*, effects of recombinant human CTGF on growth of ovarian cancer cells. Ovarian cancer cells lacking expression of *CTGF* (HNOA and HMOA) were treated with 2.5 μg/mL of recombinant human CTGF or vehicle (PBS) alone for 72 h. *Top*, cell viability was determined by WST assay in both cell lines; *bottom*, the population in each phase of cell cycle was assessed by FACS using HMOA cell line. Similar result was obtained in HNOA cell line (data not shown). *Columns*, mean of triplicate experiments; *bars*, SD. *a*, $P < 0.05$, statistical analysis used the Mann-Whitney *U* test. *C*, representative result of Western blotting for P-ERK1/2 and total ERK (ERK1/2) in HMOA cell line. HMOA cells were serum starved for 24 h, pretreated with CTGF (2.5 μg/mL) or vehicle (PBS) for 1 h, and then stimulated with EGF (25 ng/mL) of vehicle (PBS) for additional 15 min. ERK activation was evaluated by the amount of P-ERK determined by Western blotting. Similar result was obtained in HNOA cell line (data not shown). *D*, effect of knockdown of endogenous CTGF on growth of ovarian cancer cells. Fifty nanomol per liter of *CTGF*-specific siRNA (*CTGF*-siRNA) or a control siRNA for the *luciferase* gene (*Luc*-siRNA) were transfected into ovarian cancer cell lines expressing (KK and ES-2) or lacking (RMUG-S) CTGF, and the numbers of viable cells after transfection were assessed at the indicated times by WST assay. *Points*, mean of triplicate experiments; *bars*, SD. *a*, $P < 0.05$, statistical analysis used the Mann-Whitney *U* test.

aggressiveness of this disease. Further examination using a larger set of ovarian cancer cases will be needed to test our supposition that CTGF has two conflicting functions during tumorigenesis and inactivation of CTGF at least partly due to DNA methylation is a frequent and important event in the early progression of ovarian cancer.

In functional analyses, we showed that ectopically expressed CTGF or treatment with recombinant CTGF inhibits growth of *CTGF*-nonexpressing ovarian cancer cells, whereas knockdown of CTGF promotes growth of *CTGF*-expressing ovarian cancer cells. Similar results were obtained in cell lines of other types of cancer, such as NSCLC (16) and breast cancer (43). Chien et al. (16) showed that the growth of NSCLC cell lines expressing wild-type p53 was suppressed by forced expression of CTGF, likewise Cyr61, another member of the CCN family (50), although they have provided no evidence that their growth-inhibitory activity is mediated through p53. In our study, CTGF-induced growth suppression was observed in ovarian cancer cell lines regardless of the mutation status of *TP53*, and mutation of *TP53* was similarly observed in both *CTGF*-expressing and *CTGF*-nonexpressing ovarian cancer cell lines, suggesting that the growth-inhibitory activity of CTGF may not be affected by the mutation status of *TP53* in ovarian cancer. Because CTGF may exert growth-inhibiting activity at least partly through inhibition of the EGF-induced phosphorylation of ERK1/2 in NSCLC (16) and ovarian cancer (Fig. 4*C*), whereas it was shown that *CTGF* expression was inversely correlated with invasiveness/metastasis but not with cell growth in colorectal cancer (15), it is possible that CTGF affects different cellular functions in a cell- or tissue lineage–dependent manner.

Acknowledgments

Received 12/12/2006; revised 5/16/2007; accepted 5/24/2007.

Grant support: Grants-in-Aid for Scientific Research on Priority Areas and the 21st Century Center of Excellence Program for Molecular Destruction and Reconstitution of Tooth and Bone from the Ministry of Education, Culture, Sports, Science, and Technology, Japan and a grant-in-aid from Core Research for Evolutional Science and Technology of the Japan Science and Technology Corp.

The costs of publication of this article were defrayed in part by the payment of page charges. This article must therefore be hereby marked *advertisement* in accordance with 18 U.S.C. Section 1734 solely to indicate this fact.

We thank Dr. Hidetaka Katabuchi for providing the OSE-2a cell line and Ayako Takahashi and Rumi Mori for technical assistance.

References

1. Jemal A, Siegel R, Ward E, et al. Cancer Statistics, 2006. CA Cancer J Clin 2006;56:106–30.
2. Ozols RF, Bookman MA, Connolly DC, et al. Focus on epithelial ovarian cancer. Cancer Cell 2004;5:19–24.
3. Prowse A, Frolov A, Godwin AK. The genetics of ovarian cancer. In: Ozols RF, editor. American Cancer Society Atlas of Clinical Oncology. Hamilton (Ontario): B.C. Decker. Inc.; 2003. p. 49–82.
4. Friend SH, Bernards R, Rogelj S, et al. A human DNA segment with properties of the gene that predisposes to retinoblastoma and osteosarcoma. Nature 1986;323:643–6.
5. Kamb A, Gruis NA, Weaver-Feldhaus J, et al. A cell cycle regulator potentially involved in genesis of many tumor types. Science 1994;264:436–40.
6. Hahn SA, Schutte M, Hoque AT, et al. DPC4, a candidate tumor suppressor gene at human chromosome 18q21.1. Science 1996;271:350–3.
7. Jones PA, Baylin SB. The fundamental role of epigenetic events in cancer. Nat Rev Genet 2002;3:415–28.
8. Inazawa J, Inoue J, Imoto I. Comparative genomic hybridization (CGH)-arrays pave the way for identification of novel cancer-related genes. Cancer Sci 2004;95:559–63.
9. Sonoda I, Imoto I, Inoue J, et al. Frequent silencing of low density lipoprotein receptor-related protein 1B (LRP1B) expression by genetic and epigenetic mechanisms in esophageal squamous cell carcinoma. Cancer Res 2004;64:3741–7.
10. Imoto I, Izumi H, Yokoi S, et al. Frequent silencing of the candidate tumor suppressor PCDH20 by epigenetic mechanism in non-small-cell lung cancers. Cancer Res 2006;66:4617–26.
11. Katsaros D, Cho W, Singal R, et al. Methylation of tumor suppressor gene p16 and prognosis of epithelial ovarian cancer. Gynecol Oncol 2004;94:685–92.
12. Agathanggelou A, Honorio S, Macartney DP, et al. Methylation associated inactivation of RASSF1A from region 3p21.3 in lung, breast, and ovarian tumours. Oncogene 2001;20:1509–18.
13. Catteau A, Harris WH, Xu CF, Solomon E. Methylation of the BRCA1 promoter region in sporadic breast and ovarian cancer: correlation with disease characteristics. Oncogene 1999;18:1957–65.
14. Geisler JP, Goodheart MJ, Sood AK, Holmes RJ, Hatterman-Zogg MA, Buller RE. Mismatch repair gene expression defects contribute to microsatellite instability in ovarian carcinoma. Cancer 2003;98:2199–206.
15. Lin BR, Chang CC, Che TF, et al. Connective tissue growth factor inhibits metastasis and acts as an independent prognostic marker in colorectal cancer. Gastroenterology 2005;128:9–23.
16. Chien W, Yin D, Gui D, et al. Suppression of cell proliferation and signaling transduction by connective tissue growth factor in non-small cell lung cancer cells. Mol Cancer Res 2006;4:591–8.
17. Chiba T, Yokosuka O, Arai M, et al. Identification of genes up-regulated by histone deacetylase inhibition with cDNA microarray and exploration of epigenetic alterations on hepatoma cells. J Hepatol 2004;41:436–45.
18. Chiba T, Yokosuka O, Fukai K, et al. Identification and investigation of methylated genes in hepatoma. Eur J Cancer 2005;41:1185–94.
19. Hayashi H, Nagae G, Tsutsumi S, et al. High-resolution mapping of DNA methylation in human genome using oligonucleotide tiling array. Hum Genet 2007;120:701–11.
20. Kikuchi Y, Miyauchi M, Kizawa I, Oomori K, Kato K. Establishment of a cisplatin-resistant human ovarian cancer cell line. J Natl Cancer Inst 1986;77:1181–5.
21. Hirata J, Kikuchi Y, Kita T, et al. Modulation of sensitivity of human ovarian cancer cells to *cis*-diamminedichloroplatinum(II) by 12-*O*-tetradecanoylphorbol-13-acetate and DL-buthionine-S,R-sulphoximine. Int J Cancer 1993;55:521–7.
22. Watanabe T, Imoto I, Kosugi Y, et al. A novel amplification at 17q21-23 in ovarian cancer cell lines detected by comparative genomic hybridization. Gynecol Oncol 2001;81:172–7.
23. Nitta M, Katabuchi H, Ohtake H, Tashiro H, Yamaizumi M, Okamura H. Characterization and tumorigenicity of human ovarian surface epithelial cells immortalized by SV40 large T antigen. Gynecol Oncol 2001;81:10–7.
24. Saigusa K, Imoto I, Tanikawa C, et al. RGC32, a novel p53-inducible gene, is located on centrosomes during mitosis and results in G_2/M arrest. Oncogene 2007;26:1110–21.
25. Xiong Z, Laird PW. COBRA: a sensitive and quantitative DNA methylation assay. Nucleic Acids Res 1997;25:2532–4.
26. Imoto I, Tsuda H, Hirasawa A, et al. Expression of cIAP1, a target for 11q22 amplification, correlates with resistance of cervical cancers to radiotherapy. Cancer Res 2002;62:4860–6.
27. Iwabuchi H, Sakamoto M, Sakunaga H, et al. Genetic analysis of benign, low-grade, and high-grade ovarian tumors. Cancer Res 1995;55:6172–80.
28. Arnold N, Hagele L, Walz L, et al. Overrepresentation of 3q and 8q material and loss of 18q material are recurrent findings in advanced human ovarian cancer. Genes Chromosomes Cancer 1996;16:46–54.
29. Sonoda G, Palazzo J, du Manoir S, et al. Comparative genomic hybridization detects frequent overrepresentation of chromosomal material from 3q26, 8q24, and 20q13 in human ovarian carcinomas. Genes Chromosomes Cancer 1997;20:320–8.
30. Dews M, Homayouni A, Yu D, et al. Augmentation of tumor angiogenesis by a Myc-activated microRNA cluster. Nat Genet 2006;38:1060–5.
31. Berchuck A, Rodriguez GC, Kamel A, et al. Epidermal growth factor receptor expression in normal ovarian epithelium and ovarian cancer. I. Correlation of receptor expression with prognostic factors in patients with ovarian cancer. Am J Obstet Gynecol 1991;164:669–74.
32. Brigstock DR. The connective tissue growth factor/cysteine-rich 61/nephroblastoma overexpressed (CCN) family. Endocr Rev 1999;20:189–206.
33. Lau LF, Lam SC. The CCN family of angiogenic regulators the integrin connection. Exp Cell Res 1999;248:44–57.
34. Perbal B. The CCN family of genes a brief history. Mol Pathol 2001;54:103–4.
35. Perbal B. NOV (nephroblastoma overexpressed) and the CCN family of genes structural and functional issues. Mol Pathol 2001;54:57–79.
36. Kang Y, Siegel PM, Shu W, et al. A multigenic program mediating breast cancer metastasis to bone. Cancer Cell 2003;3:537–49.
37. Pan LH, Beppu T, Kurose A, et al. Neoplastic cells and proliferating endothelial cells express connective tissue growth factor (CTGF) in glioblastoma. Neurol Res 2002;24:677–83.
38. Koliopanos A, Friess H, di Mola FF, et al. Connective tissue growth factor gene expression alters tumor progression in esophageal cancer. World J Surg 2002;26:420–7.
39. Wenger C, Ellenrieder V, Alber B, et al. Expression and differential regulation of connective tissue growth factor in pancreatic cancer cells. Oncogene 1999;18:1073–80.
40. Kubo M, Kikuchi K, Nashiro K, et al. Expression of fibrogenic cytokines in desmoplastic malignant melanoma. Br J Dermatol 1998;139:192–7.
41. Shakunaga T, Ozaki T, Ohara N, et al. Expression of connective tissue growth factor in cartilaginous tumors. Cancer 2000;89:1466–73.
42. Moritani NH, Kubota S, Nishida T, et al. Suppressive effect of overexpressed connective tissue growth

factor on tumor cell growth in a human oral squamous cell carcinoma-derived cell line. Cancer Lett 2003;192: 205–14.
43. Hishikawa K, Oemar BS, Tanner FC, Nakaki T, Luscher TF, Fujii T. Connective tissue growth factor induces apoptosis in human breast cancer cell line MCF-7. J Biol Chem 1999;274:37461–6.
44. Jiang WG, Watkins G, Fodstad O, Douglas-Jones A, Mokbel K, Mansel RE. Differential expression of the CCN family members Cyr61, CTGF, and Nov in human breast cancer. Endocr Relat Cancer 2004;11:781–91.
45. Planque N, Perbal B. A structural approach to the role of CCN (CYR61/CTGF/NOV) proteins in tumourigenesis. Cancer Cell Int 2003;3:1–15.
46. Misawa A, Inoue J, Sugino Y, et al. Methylation-associated silencing of the nuclear receptor 112 gene in advanced-type neuroblastomas, identified by bacterial artificial chromosome array-based methylated CpG island amplicon. Cancer Res 2005;65:10233–42.
47. Kolb A. The first intron of the murine β-casein gene contains a functional promoter. Biochem Biophys Res Commun 2003;306:1099–105.
48. Nakagawachi T, Soejima H, Urano T, et al. Silencing effect of CpG island hypermethylation and histone modifications on *O6*-methylguanine-DNA methyltransferase (MGMT) gene expression in human cancer. Oncogene 2003;22:8835–44.
49. Deckers M, van Dinther M, Buijs J, et al. The tumor suppressor Smad4 is required for transforming growth factor β-induced epithelial to mesenchymal transition and bone metastasis of breast cancer cells. Cancer Res 2006;66:2202–9.
50. Tong X, Xie D, O'Kelly J, Miller CW, Muller-Tidow C, Koeffler HP. Cyr61, a member of CCN family, is a tumor suppressor in non-small cell lung cancer. J Biol Chem 2001;276:47709–14.

Breast Cancer
Vol. 14 No. 1 January 2007

Review Article

Sentinel Lymph Node Biopsy is Feasible for Breast Cancer Patients after Neoadjuvant Chemotherapy

Takayuki Kinoshita

Division of Surgical Oncology National Cancer Center Hospital

Background: Despite the increasing use of both sentinel lymph node (SLN) biopsy and neoadjuvant chemotherapy (NAC) in patients with operable breast cancer, information on the feasibility and accuracy of sentinel node biopsy following neoadjuvant chemotherapy is still quite limited. Therefore, we investigated the feasibility and accuracy of sentinel lymph node biopsy for breast cancer patients after NAC.

Methods: A total of 104 patients with Stage II and III breast cancers, previously treated by NAC, were enrolled in the study. All patients were clinically node-negative after NAC. The patients underwent SLN biopsy, which involved a combination of an intradermal injection of radiocolloid and a subareolar injection of blue dye over the tumor. This was followed by completion axillary lymph node dissection (ALND).

Results: SLN could be identified in 97 of 104 patients (identification rate, 93.3%). In 93 of the 97 patients (95.9%), the SLN accurately predicted the axillary status. Four patients' SLN biopsies were false negative, resulting in a false-negative rate of 10.0%. The SLN identification rate tended to be lower among patients with T4 primary tumors prior to NAC (62.5%).

Conclusion: The SLN identification and false-negative rates were similar to rates in non-neoadjuvant studies. The SLN accurately predicted metastatic disease in the axilla of patients with tumor response following NAC.

Breast Cancer 14:10-15, 2007.

Key words: Sentinel node biopsy, Neoadjuvant chemotherapy, Breast cancer, Intradermal injection

Introduction

Currently, the status of the axillary lymph nodes is the most important prognostic indicator for breast cancer and helps guide the physician in adjuvant therapy. More than 40 peer-reviewed pilot studies, published between 1993 and 1999, have established the validity of the SLN biopsy technique for clinically node-negative breast cancer[1] and SLN biopsy has become the standard of care for axillary staging in such patients.

Recent studies report identification rates greater than 90% and false-negative rates ranging from 2 to 10%[2,3]. To ensure a high SLN identification rate and a low false-negative rate, some relative contraindications for SLN biopsy have been established, including T3 or T4 tumors, multicentric or multifocal lesions, a large biopsy cavity, previous axillary surgery, previous chest-wall irradiation, and NAC[4,5].

The application of SLN biopsy in NAC patients may identify, as in non-neoadjuvant chemotherapy groups, patients who do not necessarily require an ALND. Several studies have evaluated the use of SLN biopsy in patients with breast cancer after NAC, but the results have been varied and inconclusive[6-14].

Recently, the American Society of Clinical Oncology panel concluded that there are insufficient data to recommend SLN biopsy for patients receiving preoperative therapy, although SLN biopsy after preoperative systemic chemotherapy is technically feasible[15]. It is possible that the tumor response to chemotherapy may alter or

Reprint requests to Takayuki Kinoshita, Division of Surgical Oncology National Cancer Center Hospital, 5-1-1, Tsukiji Chuo-ku, Tokyo 104-0045, Japan
E-mail: takinosh@ncc.go.jp

Abbreviations:
SLN, Sentinel lymph node; NAC, Neoadjuvant chemotherapy; ALND, Axillary lymph node dissection

interrupt the lymphatic drainage, thus causing lower SLN identification rates and higher false-negative rates than in non-neoadjuvant studies. We hypothesize that the lymphatic flow within the skin lesion overlying the tumor is less damaged by chemotherapy than that in the parenchyma surrounding the tumor, except in T4 tumors. Thus, the usefulness of SLN biopsy with intradermal radiocolloid injection for patients with NAC-treated breast cancer has yet to be established.

The objective of this study was to determine the feasibility and accuracy of SLN biopsy using intradermal radiocolloid injection over the tumor in clinically node-negative, NAC-treated breast cancer patients.

Patients and Methods

Between May 2003 and October 2005, 104 patients with T2-4N0-2 breast cancer underwent NAC with SLN biopsy plus ALND performed by a single surgeon. The pathologic diagnosis was established by core needle biopsy in all patients prior to NAC.

Patients under 65 of age received four cycles of 5FU (500mg/m^2) / epirubicin (100mg/m^2) / cyclophosphamide (500mg/m^2) (FEC), plus twelve weekly cycles of paclitaxel (80mg/m^2). Patients over 65 years of age received twelve weekly cycles of paclitaxel (80mg/m^2) alone. After NAC, we enrolled the 104 clinically node-negative patients into this study.

Lymphatic mapping was performed using a 3 ml combination of blue dye (Patent blue V®, TOC Ltd., Tokyo, Japan) and 30-80 megabecquerels of technetium-99m-labeled Phytate (Daiichi RI Laboratory, Tokyo, Japan). One day prior to surgery, the radiotracer was intradermally injected into the area overlying the tumor, while blue dye was intraoperatively injected into the subareolar site. For nonpalpable lesions, injections were performed using mammographic or ultrasonic needle localization. Sentinel lymph nodes were identified as blue stained, radioactive, or both. SLN biopsy was then followed by a standard level I/II ALND. For 32 patients, lymphscintigraphy was also performed prior to NAC, and was compared to lymphatic mapping after NAC.

All sentinel nodes were histologically evaluated by creating 3-5 mm serial sections and staining with hematoxylin and eosin (H&E). Lymph nodes submitted as part of the axillary dissection were submitted in their entirety and evaluated using standard H&E staining.

Table 1. Patient demographics

	Number of patients
Age (years)	
Mean	50.2
Range	27-77
Clinical tumor size (cm)*	
Mean	4.89
Range	2.5-12
Tumor classification*	
T2	61 (58.7%)
T3	35 (33.6%)
T4	8 (7.7%)
Lymph node status*	
N0	54 (52.0%)
N1	40 (38.5%)
N2	10 (9.5%)
Tumor type	
Invasive ductal	102 (98.1%)
Invasive lobular	2 (1.9%)
Type of NAC	
FEC plus paclitaxel	100 (96.2%)
paclitaxel alone	4 (3.8%)
Clinical response of the tumor	
CR	55 (52.9%)
PR	41 (39.4%)
SD	8 (7.7%)
Pathological response of the tumor	
pCR	23 (22.1%)
pINV	81 (77.9%)
Pathological nodal status	
Negative	60 (57.7%)
Positive	44 (42.3%)

*Before NAC.
pCR = pathological complete response; pINV = pathological invasive.
CR = Complete response; PR = Partial response; SD= Stable disease

Results

The patient characteristics, type of chemotherapy, clinical response of the tumor, and pathological findings are summarized in Table 1. All patients underwent breast-conserving therapy or mastectomy and were clinically node-negative at the time of operation.

Based on lymphscintigraphy studies before and after NAC, the results of lymphatic mapping were quite similar in 30/32 patients, as shown in Fig 1. SLN were not detected in two cases with a

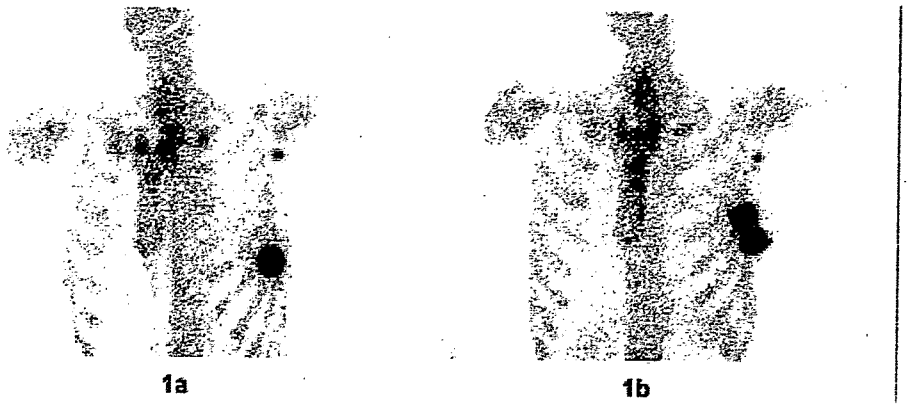

1a 1b

Fig 1. Lymphscintigraphy before and after NAC (1a and 1b, respectively) revealed one sentinel node at the axilla. The bone scintigram was performed simultaneously to detect bone metastasis.

Table 2. Results of sentinel node biopsy

	Number of patients
Total no. of patients	104
SLN identified	97 (93.4%)
SLN positive	36 (34.6%)
SLN was only positive lymph node	16 (44.4%)
SLN identification method	
Radiocolloid and blue dye	91 (87.5%)
Blue dye only	13 (12.5%)

Table 3. Comparison of lymph node status of SLNs and non-SLNs (n=97)

	Non-SLN status	
SLN status	Positive	Negative
Positive	20	16
Negative	4	57

False-negative rate, 10%; overall accuracy, 96%; negative predictive value, 93%; positive predictive value, 100%

T4d primary tumor.

As seen in Table 2, the overall SLN identification rate was 93.4% (97 of 104). Of the 97 patients in whom an SLN could be identified, 36 (34.6%) had positive SLNs. In 16 of these patients (44.4%), the SLN was the only positive node. SLNs were identified by both radiocolloid and blue dye in 91 patients (87.5%) and by blue dye alone in 13 patients (12.5%).

The pathological status of the SLNs and non-SLNs is outlined in Table 3.

The SLNs accurately predicted axillary status in 93/97 patients (95.9%). Four patients had false-negative SLN biopsies, a false-negative rate of 10.0% (4/40). Fifty-seven patients had pathologically negative SLN or non-SLN.

Table 4. Comparison of lymph node status of SLNs and non- SLNs among tumor classifications before NAC

	T2 (n=59)		T3/T4 (n=38)	
	Non- SLN status			
SLN status	Positive	Negative	Positive	Negative
Positive	7	7	13	9
Negative	2	43	2	14
	SLN identified, 59/61 (97%) False-negative rate, 13%		SLN identified, 38/43 (88%) False-negative rate, 8%	

The pathological status of the SLNs and non-SLNs was analyzed according to tumor classifications before NAC, clinical lymph node status before NAC, and the response of the tumor after NAC.

In T2 tumors before NAC, the SLN identification rate was 97% (59 of 61), and 2 patients had false-negative SLN biopsies, or a false-negative rate of 13%. In T3 and T4 tumors, the results were 88.4% (38 of 43) and 8%, respectively (Table 4). The SLN identification rate tended to be higher in patients with a T2 primary tumor before NAC than in those with T3/T4 primary tumor before NAC, but the difference was not statistically significant.

In the SLN biopsy results, there was no significant difference between nodal status prior to NAC.

Table 5. Comparison of lymph node status of SLNs and non- SLNs among nodal status before NAC

	N0 (n=52)		N1/N2 (n=45)	
	Non- SLN status			
SLN status	Positive	Negative	Positive	Negative
Positive	4	8	16	8
Negative	2	38	2	19
	SLN identified, 52/54 (96%) False-negative rate, 14%		SLN identified, 45/50 (90%) False-negative rate, 7%	

Table 6. Comparison of lymph node status of SLNs and non- SLNs among clinical response after NAC

	CR (n=50)		PR/SD (n=47)	
	Non- SLN status			
SLN status	Positive	Negative	Positive	Negative
Positive	6	5	14	11
Negative	2	37	2	20
	SLN identified, 50/55 (91%) False-negative rate, 15%		SLN identified, 47/49 (96%) False-negative rate, 7%	

Table 7. Success rate of sentinel node identification according to tumor characteristics

	No. of Attempted	Success Rate (%)	P
Tumor classification			
T2	61	97 %	*N.S.*
T3	35	94 %	
T4	8	63 %	
Clinical nodal status			
Negative	54	96 %	*N.S.*
Positive	50	90 %	
Clinical tumor response			
CR	55	91 %	*N.S.*
PR/SD	49	96 %	
Pathological tumor response			
pCR	23	91%	*N.S.*
pINV	81	94 %	

In the patients with clinically negative lymph nodes (N0) before NAC, the SLN identification rate was 96.3% (52 of 54), and two patients had a false-negative SLN biopsy, a false-negative rate of 14%. In the patients with clinically positive lymph nodes (N1/N2), the results were 90% (45 of 50) and 7%, respectively (Table 5). In the SLN biopsy results, there was no significant difference between nodal status prior to NAC.

For patients with complete tumor response (CR) after NAC, the SLN identification rate was 91.0% (50/55) and two patients had false-negative SLN biopsies, resulting in a false-negative rate of 15%. For patients with partial tumor response (PR) and stable disease (SD), the results were 96.0% (47/49) and 7%, respectively (Table 6). The SLN identification rate tended to be lower, although the difference was not statistically significant, after NAC in patients with CR after NAC as compared to those with PR and SD.

There was no significant difference in the false-negative rate according to the tumor classification before NAC, the clinical lymph node status before NAC, or the tumor responses after NAC.

There was also no significant difference in the success rate of SLN identification according to tumor classifications before NAC, the clinical lymph node status before NAC, the clinical response of the tumor after NAC, or the pathological response of the tumor after NAC, although the success rate tended to be lower in patients with a T4 primary tumor (Table 7).

Discussion

Although the use of SLN biopsy has dramatically increased over the past several years, and some experienced surgeons are performing this procedure without completing axillary dissection, it is unlikely that SLN biopsy will become the generally accepted standard of care in axillary staging until results from ongoing randomized trials

Table 8. Studies of SLN biopsy after NAC

	No. of patients	Stage	Tumor size (cm)	No (%) of successful SLN biopsies	False negative (%)
Breslin et al.,2000 [6]	51	II or III	5.0	43 (84.3)	3 (12)
Miller et al., 2002 [7]	35	T1-3N0	3.5	30 (86.0)	0 (0)
Stearns et al.,2000 [8]	34	T3-4, any N	5.0	29 (85.0)	3 (14)
Haid et al.,2001 [9]	33	T1-3, any N	3.3	29 (88.0)	0 (0)
Julian et al.,2002 [10]	31	I or II	NS	29 (93.5)	0 (0)
Tafra et al.,2001 [12]	29	Any T, N0	NS	27 (93.0)	0 (0)
Nason et al.,2000 [13]	15	T2-4, N0	NS	13 (87.0)	3 (33)
Shimazu et al.,2004 [14]	47	II or III	4.5	44 (93.6)	4 (12)
Current study	104	T2-4, any N	4.9	97 (93.0)	4 (10)

demonstrate the equivalence of this procedure with axillary dissection in terms of axillary recurrence and overall survival. At the same time, it is unlikely that the value of sentinel node biopsy following NAC will be established[1]. The main reason for this is that only a small proportion of operable breast cancer patients currently receive NAC, making a randomized trial quite difficult. Another reason is that when the results from the ongoing randomized trials are disclosed, if they are favorable towards the SLN biopsy procedure, the majority of surgeons will extrapolate the applicability of these results to patients who have received NAC. Thus, it is quite possible that demonstrating the feasibility and efficacy of SLN biopsy after NAC will depend on the retrospective data of single-institution experiences.

NAC can reduce tumor size and significantly increase the ability to perform breast-conserving therapy[16-18]. After NAC, axillary downstaging is similarly affected. NAC with anthracycline/cyclophosphamide-containing regimens has been shown to neutralize the involved axillary nodes in about 30% of patients[16]. The addition of taxanes to anthracycline/cyclophosphamide-containing regimens has increased the conversion rate to around 40%[19, 20]. With the number of patients receiving NAC increasing, the question arises as to whether SLN biopsy is an option for these patients. We summarize the studies regarding SLN biopsy after NAC in Table 8, but they are inconclusive[6-14]. Breslin *et al.*[5] reported a study of 51 patients who underwent SLN biopsy after NAC and concluded that SLN biopsy following NAC is accurate. They had an identification rate of 84.3% and a false-negative rate of 12.0%. Nason *et al.*[13] reported a smaller number of patients who hard received NAC, and their identification and false-negative rates were 87.0% and 33.3%, respectively. They concluded that SLN biopsy resulted in an unacceptably high false-positive rate. However, in these small series, even 1 or 2 patients with false-negative SLNs can greatly affect the conclusions in a different direction. We report here a study of 104 patients who received NAC and had an identification rate of 93.4% and false-negative rate of 10.0%. We conclude in our study that SLN biopsy after NAC is accurate and feasible even for large tumors and patients with positive axillary nodal status before NAC without inflammatory breast cancer.

It has been speculated that among patients who have had their axillary lymph node status downstaged by NAC, tumors also typically respond to NAC and shrink so that damage to and alteration of the lymphatic flow from tumor tissues to the axillary basin are more likely to occur. This might then cause an increased false-negative rate for SLN biopsy and a decreased identification rate of SLN biopsy. However the hypothesis of the present study is that the lymphatic flow around skin lesions is rich and less influenced by the effects of chemotherapy and tumor size than that in the parenchyma surrounding the tumor. The lymphscintigraphy in this study results before and after NAC demonstrated that the effect of NAC did not at all change the lymphatic flow of the breast.

The results of our study suggest that SLN biopsy after NAC using intradermal injection of radiocolloid is feasible and can accurately predict axillary lymph node status for patients with clinically negative lymph node status following NAC. This procedure could help patients who have had their

axillary lymph node status downstaged from positive to negative and patients with large tumors qualify as appropriate candidates for SLN biopsy.

Further, multicenter studies, involving a larger number of patients from a variety of clinical locations, will be required to fully establish the feasibility and accuracy of SLN biopsy for patients with breast cancer who have been treated with NAC.

References

1) Cody HS 3rd: Clinical aspects of sentinel node biopsy. *Breast Cancer Res* 3:104-1088. 1B, 2001.
2) Cody HS, Borgen PI: State-of-the-art approaches to sentinel node biopsy for breast cancer: study design, patient selection, technique and quality control at Memorial Sloan-Kettering Cancer Center. *Surg Oncol* 8:85-91, 1999.
3) Krag D, WeaverD, Ashikaga T, Moffat F, Klimberg VS, Shriver C, Feldman S, Kusminsky R, Gadd M, Kuhn J, Harlow S, Beitsch P: The sentinel node in breast cancer-a multicenter validation study. *N Engl J Med* 339:941-946, 1998.
4) Anderson BO: Sentinel lymphadenectomy in breast cancer: an update on NCCN Clinical Practice Guidelines. *J Natl Compr Cancer Network* 1 Suppl 1:S64-70, 2003.
5) Reintgen D, Giuliano R, Cox C: Lymphatic mapping and sentinel lymph node biopsy for breast cancer. *Cancer J* 8 Suppl 1:S15-21, 2002.
6) Breslin TM, Cohen L, Sahin A, Fleming JB, Kuerer HM, Newman LA, Delpassand ES, House T, Ames FC, Feig BW, Ross MI, Singgletary SE, Buzdar AU, Hortobagyi GN, Hunt KK: Sentinel lymph node biopsy in accurate after neoadjuvant chemotherapy for breast cancer. *J Clin Oncol* 18:3480-3486, 2000.
7) Miller AR, Thompson VE, Yeh IT, Alrakwan A, Sharkey FE, Stauffer J, Otto PM, Mckay C, Kahlenberg MS, Phillips WT, Cruz AB Jr: Analysis of sentinel lymph node mapping with immediate pathologic review in patients receiving preoperative chemotherapy for breast carcinoma. *Ann Surg Oncol* 9:243-247, 2002.
8) Stearns V, Ewing CA, Slake R,Panannen MF, Hayes DF, Tsangaris TN: Sentinel lymphadenectomy after neoadjuvant chemotherapy for breast cancer may reliably represent the axilla except for inflammatory breast cancer. *Ann Surg Oncol* 9: 235-242, 2000.
9) Haid A, Tausch C, Lang A, Lutz J, Fritzsche H, Prschina W, Breitfellner G, Sege W, Aufschnaiter M, Sturn H, Zimmermann G: Is sentinel lymph node biopsy reliable and indicated after preoperative chemotherapy in patients with breast carcinoma? *Cancer* 92:1080-1084, 2001.
10) Julian TB, Patel N, Dusi D, Olson P, Nathan G, Jasnosz K, Isaacs G, Wolmark N: Sentinel node biopsy after neoadjuvant chemotherapy for breast cancer. *Am J Surg* 182:407-410, 2001.
11) Julian TB, Dusi D, Wolmark N: Sentinel node biopsy after neoadjuvant chemotherapy for breast cancer. *Am J Surg* 184:315-317, 2002.
12) Tafra L, Verbanac KM, Lannin DR: Preoperative chemotherapy and sentinel lymphadenectomy for breast cancer. *Am J Surg* 182:312-315, 2001.
13) Nason KS, Anderson BO, Byrd DR, Dunnwald LK, Eary JF, Mankoff DA, Livingston R, Schimidt RA, Jewell KD, Yeung RS, Moe RE: Increased false negative sentinel node biopsy rates after preoperative chemotherapy for invasive breast carcinoma. *Cancer* 89:2187-2194, 2000.
14) Shimazu K, Tamaki Y, Taguchi T, Akazawa K, Inoue T, Noguchi S: Sentinel lymph node biopsy using periareolar injection of radiocolloid for patients with neoadjuvant chemotherapy-treated breast carcinoma. *Cancer* 100:2555-2561, 2004.
15) Lyman GH, Giuliano AE, Somerfield MR, Bensen AB, Bodurka DC, Burstein HJ, Cochran AJ, Cody III HS, Edge SB, Galper S, Hayman JA, Kim TY, Perkins CL, Podoloff DA, Sivausbramaniam VH, Turner RR, Wakl R, Weaver RW, Wolff CA, Winer EP: American Society of Clinical Oncology guideline recommendations for sentinel lymph node biopsy in early-stage breast cancer. *JCO* 23:2540-2545, 2005.
16) Fisher B, Brown A, Mamounas E, Wieand S, Robidoux A, Margolese RG, Cruz AB Jr, Fisher ER, Wicferham DL, Wolmark N, DeCillis A, Hoehn JL, Lees AW Dimitrov NV: Effect of preoperative chemotherapy on local-regional disease in women with operable breast cancer: findings from the National Surgical Adjuvant Breast and Bowel Project B-18. *J Clin Oncol* 15:2483-2493, 1997.
17) Hutcheon AW, Heys SD, Miller ID: Improvements in survival in patients receiving primary chemotherapy with docetaxel for breast cancer: a randomized control trial. Presented at the 24th Annual San Antonio Breast Cancer Symposium. San Antonio, Texas, December 2001.
18) O'Hea BJ, Hill AD, El-Shirbiny AM, Yeh SD, Rosen PP, Coit DG, Borgen PI, Cody HS 3rd: Sentinel lymph node biopsy in breast cancer: Initial experience at Memorial Sloan-Kettering Cancer Center. *J Am Coll Surg* 186:423-427, 1998.
19) Mamounaus E, Brown A, Smith R: Accuracy of sentinel node biopsy after neoadjuvant chemotherapy in breast cancer: update results from NSABP B-27. *Proc Am Soc Clin Oncol* 21:36a, 2002.
20) Gianni L, Baselga H, Eiermann W: First report of European Cooperative Trial in operable breast cancer (ECTO): effect of primary systemic therapy (PST) on local-regional disease. *Proc Am Soc Clin Oncol* 21:34a, 2002.

Breast Cancer
Vol. 14 No. 4 October 2007

Case Report

Brain Metastases after Achieving Local Pathological Complete Responses with Neoadjuvant Chemotherapy

Shunsuke Tsukamoto, Sadako Akashi-Tanaka, Tadahiko Shien, Kotoe Terada, Takayuki Kinoshita

Breast Surgery Division, National Cancer Center hospital, Tokyo, Japan

Background: We encountered two patients with inflammatory breast carcinoma who developed symptomatic brain metastases after achieving local pathological complete responses (pCR) with neoadjuvant chemotherapy (NAC).

Case presentations: The first patient is a 39-year-old woman (Case 1), who underwent NAC with AC (doxorubicin + cyclophosphamide) followed by weekly paclitaxel. After achieving a clinical CR (cCR), we conducted a modified radical mastectomy. Pathological evaluation confirmed no residual malignant cells within the breast tissue or lymph nodes. However, she developed neurological symptoms from brain metastases one month postoperatively. The second patient is a 44-year-old woman (Case 2). Again, no residual malignant cells were detected within the breast tissue or lymph nodes following NAC, but the patient developed symptomatic brain metastases eight months postoperatively. When primary breast tumors are locally advanced, it may be worthwhile to rule out brain metastases even if pCR is obtained after NAC.

Breast Cancer 14:420-424, 2007.

Key words: Brain metastasis, Pathological complete response, Breast cancer

Introduction

Neoadjuvant chemotherapy (NAC) is a standard treatment option for patients with locally advanced and/or inflammatory breast cancers. The outcomes of patients achieving pCR of their primary tumors are significantly better than those with residual disease[1-3]. Here, we introduce two patients who developed symptomatic brain metastases shortly after documented pCRs following NAC and surgery.

Case Report

Case 1

A 39-year-old premenopausal woman sought medical attention for erythematous induration of her left breast. With a working diagnosis of inflammatory breast cancer, fine needle aspiration cytology revealed adenocarcinoma. The patient was referred to the National Cancer Center Hospital for further treatment in February 2005. Physical examination revealed an indistinct 12 cm mass in the upper area of the left breast, and the surface of this lesion exhibited a peau d'orange appearance. Axillary and supraclavicular lymph nodes were palpable and measured 4 and 2 cm in diameter, respectively. The axillary lymph node was fixed to the surrounding tissue. Ultrasonography (US) revealed a 7 cm breast mass with dermal thickening, edematous subcutaneous tissue, and enlarged lymph nodes (Fig 1a). These findings were also observed on computed tomography (CT) and magnetic resonance imaging (MRI).

Core needle biopsy led to a pathological diagnosis of invasive ductal carcinoma (grade 3, nuclear grade 3, and HER-2 negative) (Fig 2a). The tumor was negative for both estrogen and progesterone receptors. Chest X-ray, bone scintigraphy, abdominal US, and chest and abdominal CT revealed no distant metastases. Due to the presumed low incidence of brain metastases at this clinical stage, brain imaging was not done at

Reprint requests to Sadako Akashi-Tanaka, Breast surgery division, National Cancer Center hospital, 5-1-1 Tsukiji, Chuo-ku, Tokyo, 104-0045, Japan.

Abbreviations:
pCR, Pathological complete response; NAC, neoadjuvant chemotherapy; US, ultrasonography; CT, Computed tomography; MRI, Magnetic resonance imaging

Received September 11, 2006; accepted May 14, 2007

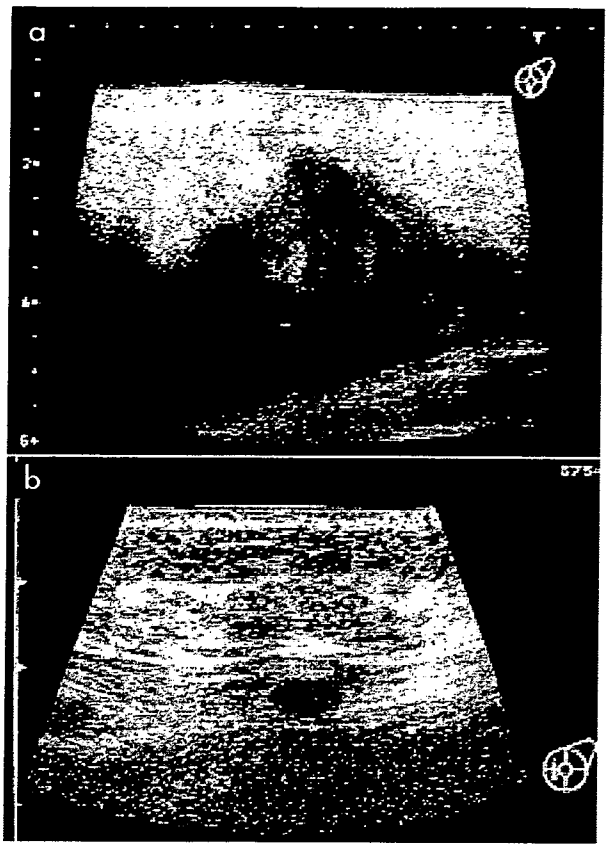

Fig 1. (a) US reveals a 7 cm breast mass with overlying skin thickening, edematous subcutaneous tissue. (b) US reveals no residual tumor following neoadjuvant chemotherapy.

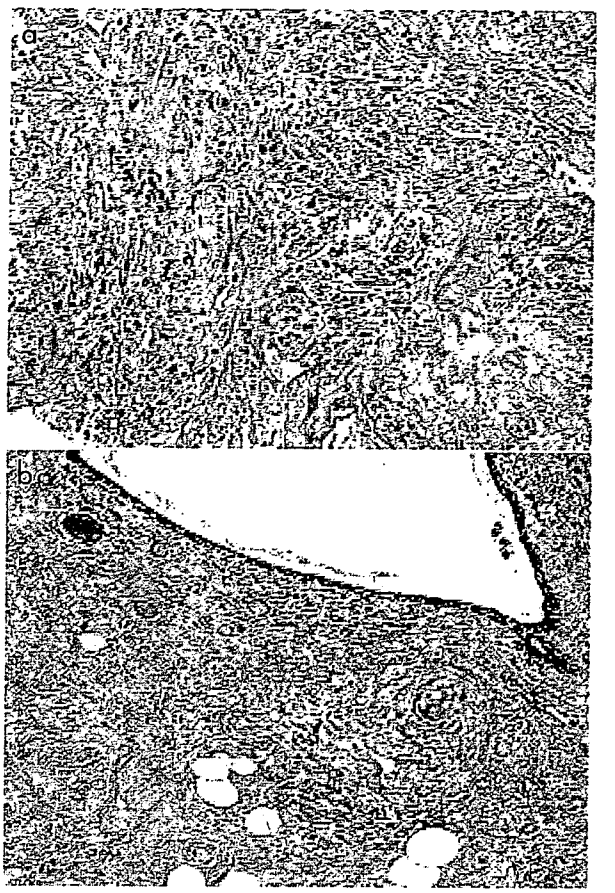

Fig 2. (a) Core needle biopsy reveals invasive ductal carcinoma, grade 3, nuclear grade 3. (b) No residual tumor is detected. The presence of inflammatory cells surrounding a duct with an increased number of enlarged capillary vessels, typical after tumor disappearance, is observed. (hematoxylin-eosin staining, ×100).

this point. Inflammatory breast cancer of the left breast was initially diagnosed, T4dN3M0, Stage IIIC, according to the general rules for clinical and pathological grading of breast cancers[4]. She received NAC from February to July consisting of doxorubicin and cyclophosphamide (60/600 mg/m^2) 4 times every 3 weeks, followed by paclitaxel (80 mg/m^2) weekly for 12 weeks. Following NAC, only induration of her left breast was apparent upon physical examination, and no breast masses or axillary lymph nodes were detected by US (Fig 1b) and CT. Additionally, serum levels of tumor markers (CEA, CA 15-3, ST 439) remained within normal limits before and after chemotherapy. We subsequently conducted a modified radical mastectomy in August, and no malignant cells were detected in the resected breast tissue and dissected axillary lymph nodes (Fig 2b). However, the patient presented with vertigo and severe headache prior to the initiation of radiotherapy to the left chest wall in September. Brain MRI revealed multiple metastatic lesions in her right frontal lobe, temporal lobe, and bilateral cerebellum (Fig 3). To control her symptoms, whole-brain radiotherapy with a total dose of 30 Gy/10 fractions was incorporated in October. However, her condition deteriorated, and she expired in December.

Case 2

A 44-year-old premenopausal woman was seen at a nearby hospital with a chief complaint of an erythematous enlarged right breast. Inflammatory breast cancer was suspected, so she was referred to our institution in December 2004.

On initial examination, the right breast was firm, erythematous, and edematous with a thickened dermis. Axillary and supraclavicular lymph nodes were palpable and measured 5 cm and 1 cm

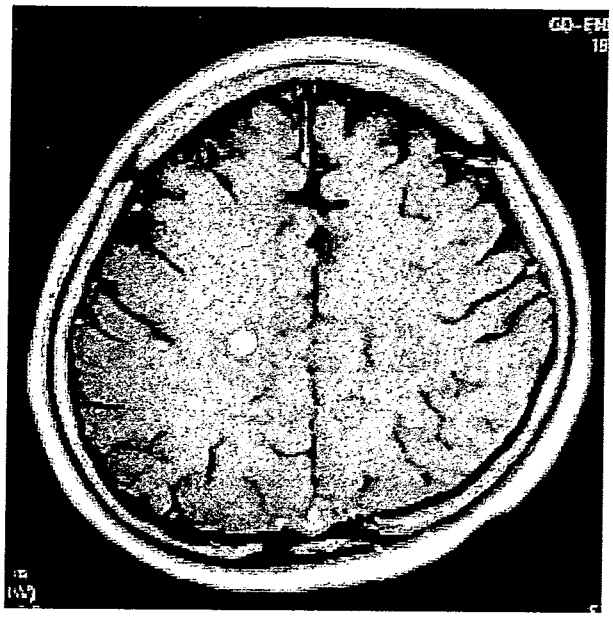

Fig 3. The metastatic lesions exhibited high signal intensity in the right temporal lobe by T1 weighted MRI.

in diameter, respectively. CT showed a large right breast mass with an edematous dermis and subcutaneous tissue.Additionally, the axillary and supraclavicular lymph nodes were enlarged (Fig 4a). The specimen obtained by the core needle biopsy was consistent with an invasive ductal carcinoma (solid tubular type, grade 3, nuclear grade 3, HER-2 negative, estrogen and progesterone receptor negative) (Fig 5a). No metastatic lesions were detected by bone scintigraphy, chest X-ray, chest CT, or abdominal US, though diagnostic brain imaging was not performed at that time. Serum tumor markers were elevated, with a CEA of 52.4 ng/ml, CA 15-3 of 279 U/ml, and NCC-ST 439 of 910 U/ml. Inflammatory breast cancer, T4dN3M0, Stage IIIC[4] was diagnosed. She underwent NAC from December to May 2005, using the same treatment regimen as Patient 1. Following NAC, physical examination revealed only induration of the right breast with slight thickening of the overlying skin. CT revealed a slightly enhanced, 3-cm lesion in the breast (Fig 4b) without enlarged lymph nodes. All tumor markers were within normal limits after chemotherapy. We performed a modified radical mastectomy in July, and no tumor cells were pathologically detected in the breast tissue and axillary lymph nodes (Fig 5b). Following surgery, we performed local radiotherapy with a total dose of 60 Gy/30 fractions from August through October. However, the patient developed

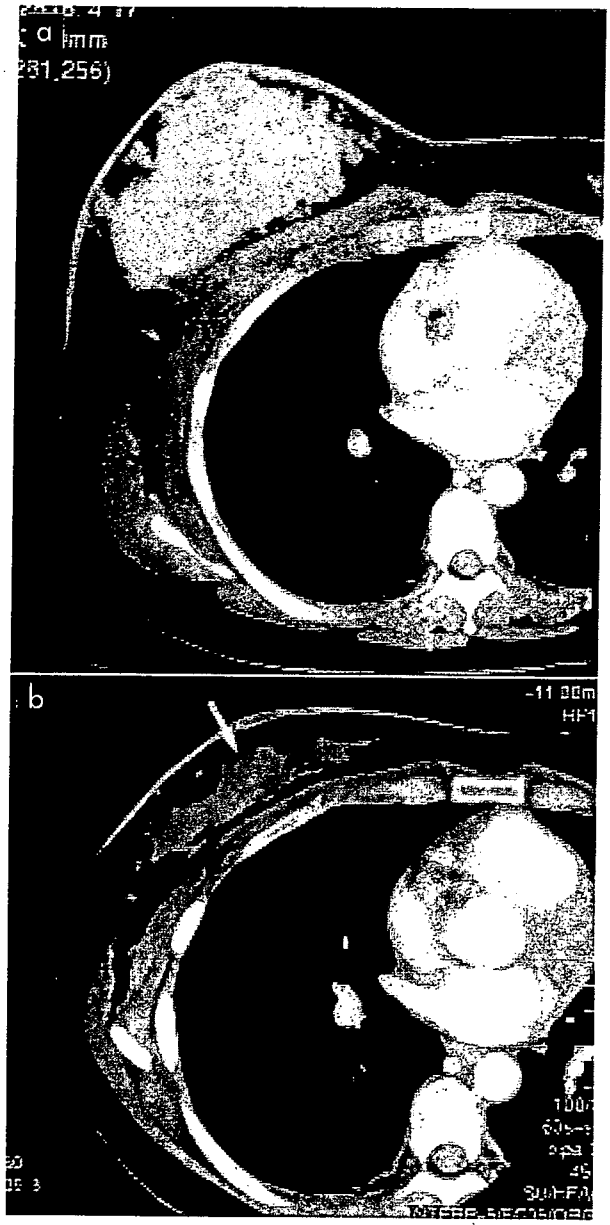

Fig 4. (a) CT shows a large right breast mass with overlying edematous subcutaneous tissue and thickened skin. This is not the early phase but late phase scan of breast CT, because only chest CT without an early phase scan was performed to detect distant metastasis instead of breast CT. (b) CT scan reveals a mass-like lesion measuring 3 cm, without enhancement, in the right breast.

headache and ambulatory disturbance in early December. Brain CT and MRI scans performed in March 2006 detected a tumor measuring 5 cm in diameter in her right temporal lobe with surrounding edema (Fig 6). A right frontotemporal craniotomy followed by whole-brain radiotherapy of 37.5 Gy/15 fractions was carried out from

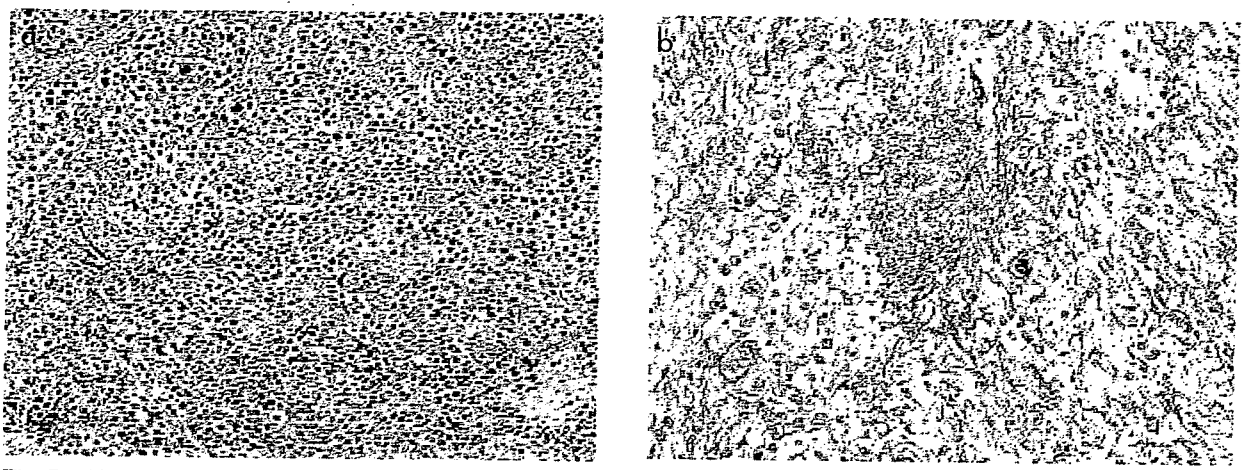

Fig 5. (a) Core needle biopsy reveals invasive ductal carcinoma, grade 3, nuclear grade 3. (b) No residual tumor is detected. Many foamy cells and a disturbance of the fiber rows after the disappearance of the tumor are observed (hematoxylin and eosin staining, ×100).

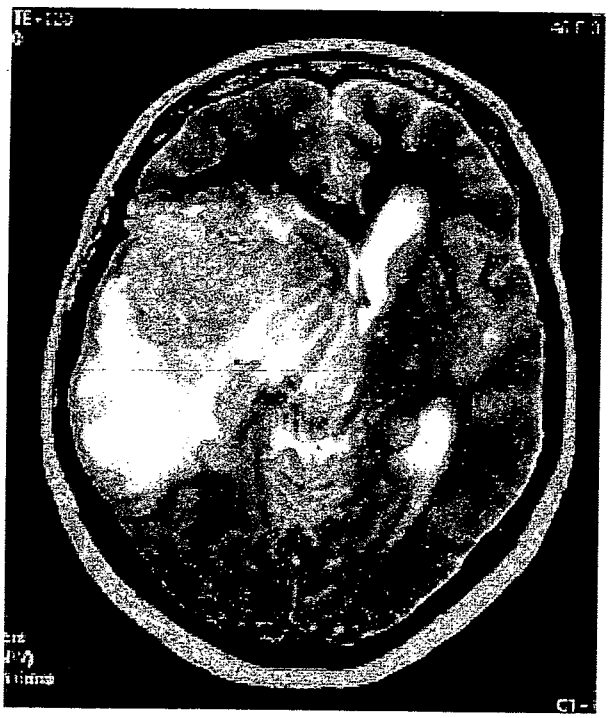

Fig 6. MRI demonstrates a tumor measuring 5 cm in diameter, with surrounding edema, in the right temporal lobe.

March through April. Intracranial recurrence is now controlled three months after radiotherapy.

Discussion

Several studies have indicated that breast cancer patients with pCR following NAC have better overall survival and disease-free survival rates[1-3]. Moreover, pCR of axillary lymph nodes is an excellent prognostic factor for locally advanced breast cancers[5-8]. The two cases presented were first diagnosed with inflammatory breast cancer with axillary and supraclavicular lymph node metastases. The patients achieved pCR for both the main tumors and the axillary lymph nodes following NAC, and favorable prognoses were expected from the published literature. However, both patients developed symptomatic brain metastases soon after mastectomy. The interval between surgery and the occurrence of neurological signs was only one month for Patient 1 and five months for Patient 2. This led us to the theory that the blood brain barrier restricted access of the chemotherapeutic agents to the central nervous system. Therefore despite locally effective NAC, occult brain metastases may continue to progress into clinical significance. This theory may help us understand the progression of brain metastases in these patients[9]. There have been no reports examining the rates of brain metastasis following NAC. Yet there are reports of patients receiving adjuvant chemotherapy having an increased incidence of brain metastases as the site of first recurrence compared to control[10, 11]. In the present cases, we suspect that subclinical metastases were present in the brain before initiating NAC. It is likely that, because of inadequate delivery of cytotoxic agents to the brain, these metastases continued to grow despite effective tumor control elsewhere the body.

Several studies have identified risk factors for brain metastases in patients with breast cancer. Young age[12, 13], unresponsiveness to the hormonal

therapies, and HER-2 over expression are reported risk factors[14-17]. Intracranial metastases are also related to the use of trastuzumab[18]. In the two patients presented here, relatively young age and the absences of both estrogen and progesterone receptor were concordant risk factors for developing brain metastases.

The combination of NAC and surgery can lead to favorable outcomes in many cases of breast cancer, but effective control over the primary lesions and the extracranial micrometastases by the cytotoxic agents may not predict future intracranial event. The blood brain barrier would likely prevent chemotherapeutic agents from reaching the central nervous system. As a consequence, brain metastases may continue to grow and become symptomatic despite pCR of primary sites and lymph node metastases. This can be a concerning factor, especially in patients at risk for developing brain metastases. Further investigations are warranted to identify the mechanisms leading to intracranial metastases, as well as pretherapeutic risk factors.

References

1) Fisher B, Bryant J, Wolmark N, Mamounas E, Brown A, Fisher R, Wickerham L, Begovic M, DeCillis A, Robidoux A, Margolese G, Cruz B, Hoehn L, Lees W, Dimitrov V, Bear D: Effect of preoperative chemotherapy on the outcome of woman with operable breast cancer. *J Clin Oncol* 16: 2672-2685, 1998.
2) Norman W, Jiping W, Eleftherios M, John B, Bernard F: Preoperative chemotherapy in patients with operable breast cancer: nine-year results from national surgical adjuvant breast and bowel project B-18. *J Natl Cancer Inst Monogr* 30: 96-102, 2001.
3) Sataloff D, Mason B, Prestipino A, Seinige U, Lieber C, Baloch Z: Pathologic response to induction chemotherapy in locally advanced carcinoma of the breast: A determinant of outcome. *J Am Coll Surg* 180: 297-306, 1995.
4) Sakamoto G, Inaji H, Akiyama F, Haga S, Hiraoka M, Inai K, Iwase T, Kobayashi S, Sakamoto G, Sano M, Sato T, Sonoo H, Tsuchiya S, Watanabe T; The Japanese Breast Cancer Society: General rules for clinical and pathological recording of breast cancer 2005. *Breast cancer* 12 (Suppl): S1-27, 2005.
5) Hennessy T, Hortobagyi N, Rouzier R, Kuerer H, Sneige N, Buzdar U, Kau W, Fornage B, Sahin A, Broglio K, Singletary E, Valero V: Outcome after pathologic complete eradication of cytologically proven breast cancer axillary node metasteses following primary chemotherapy. *J Clin Oncol* 23: 9304-9311, 2005.
6) Rouzier R, Extra M, Klijanienko J, Falcou C, Asselain B, Salomon V, Vielh P, Bourstyn E: Incidence and prognostic significance of complete axillary downstaging after primary chemotherapy in breast cancer patients with T1 to T3 tumors and cytologically proven axillary metastic lymph nodes. *J Clin Oncol* 20: 1304-1310, 2002.
7) Hennessy T, Gonzalez-Angulo M, Hortobagyi N, Cristofanilli M, Kau W, Broglio K, Fornage B, Singletary E, Sahin A, Buzdar A, Valero V: Disease-free and overall survival after pathologic complete disease remission of cytologically proven inflammatory breast carcinoma axillary lymph node metastases after primary systemic chemotherapy. *Cancer* 106: 1000-1006, 2006.
8) Kuerer M, Newman A, Smith L, Ames C, Hunt K, Dhingra K, Theriault L, Singh G, Binkley M, Sneige N, Buchholz A, Ross I, McNeese D, Buzdar U, Hortobagyi N, Singletary E: Clinical course of breast cancer patients with complete pathologic primary tumor and axillary lymph node response to doxorubicin-based neoadjuvant chemotherapy. *J Clin Oncol* 17: 460-469, 1999.
9) Freilich J, Seidman D, DeAngelis M: Central nervous system progression of metastatic breast cancer in patients treated with paclitaxel. *Cancer* 76: 232-236, 1995.
10) Paterson G, Agarwal M, Lees A, Hanson J, Szafran O: Brain metastases in breast cancer patients receiving adjuvant chemotherapy. *Cancer* 49: 651-654, 1982.
11) Crivellari D, Pagani O, Veronesi A, Lombardi D, Nole F, Thurlimann B, Hess D, Borner M, Bauer J, Martinelli G, Graffeo R, Sessa C, Goldhirsch A: High incidence of central nervous system involvement in patients with metastatic or locally advanced breast cancer treated with epirubicin and docetaxel. *Ann Oncol* 12: 353-356, 2001.
12) DiStefano A, Yap Y, Hortobagyi N, Blumenschein R: The natural history of breast cancer patients with brain metastases. *Cancer* 44: 1913-1918, 1979.
13) Tsukada Y, Fouad A, Pickren W, Lane W: Central nervous system metastasis from breast carcinoma: autopsy study. *Cancer* 52: 2349-2354, 1983.
14) Slimane K, Andre F, Delaloge S, Dunant A, Perez A, Grenier J, Massard C, Spielmann M: Risk factors for brain relapse in patients with metastatic breast cancer. *Ann Oncol* 15: 1640-1644, 2004.
15) Clark M, Sledge W, Osborne K, McGuire L. Survival from first recurrence: relative importance of prognostic factors in 1,015 breast cancer patients. *J Clin Oncol* 5: 55-61, 1987.
16) Miller D, Weathers T, Haney G, Timmerman R, Dickler M, Shen J, Sledge W: Occult central nervous system involvement in patients with metastatic breast cancer: prevalence, predictive factors and impact on overall survival. *Ann Oncol* 14: 1072-1077, 2003.
17) Bendell C, Domchek M, Burstein J, Harris L, Younger J, Kuter I, Bunnell C, Rue M, Gelman R, Winer E: Central nervous system metastases in women who receive trastuzumab-based therapy for metastatic breast carcinoma. *Cancer* 97: 2972-2977, 2003.
18) Matsumoto K, Shimizu C, Fujiwara Y: The next step to approaching central nervous system metastasis in HER-2-positive metastatic breast cancer patients. *Asia-Pac J Clin Oncol* 2: 6-8, 2006.